Journal of Foraminiferal Research, v. 38, no. 2, p. 162–182, April 2008

CHRONOSTRATIGRAPHIC FRAMEWORK FOR UPPER CAMPANIAN-MAASTRICHTIAN SEDIMENTS ON THE BLAKE NOSE (SUBTROPICAL NORTH ATLANTIC)

BRIAN T. HUBER[1,4], KENNETH G. MACLEOD[2] AND NATALIYA A. TUR[3]

ABSTRACT

A new chronostratigraphic framework is presented for upper Campanian-Maastrichtian pelagic sediments cored at DSDP/ODP Sites 390A/1049, 1050, and 1052, which were drilled across a 1300-m depth transect on the Blake Nose (subtropical western Atlantic Ocean). The planktonic foraminiferal zonation is based on standard global biozones for this interval, but rare and sporadic occurrence of two zonal biomarkers, *Gansserina gansseri* and *Globotruncana aegyptiaca*, precludes reliable identification of the nominate zones for those species. The *Pseudoguembelina palpebra* Partial-range Zone is defined as a means of subdividing this upper Campanian biostratigraphic interval. Planktonic foraminiferal, calcareous nannofossil and paleomagnetic datums are integrated to construct reliable age-depth curves for each of the Blake Nose drill sites. These age models are largely confirmed by Sr-isotopic data and suggest significant unconformities at various positions within the sections. Compilation of stable isotope datasets for this time interval from the Blake Nose sites reveals no significant shifts in $\delta^{18}O$ and $\delta^{13}C$ at the time of the inoceramid bivalve extinction (now dated as 68.5–68.7 Ma in the Blake Nose sections) and no correlation with proposed Campanian-Maastrichtian glacial intervals. However, benthic warming associated with Deccan volcanism during the late Maastrichtian is supported.

INTRODUCTION

Late Campanian through Maastrichtian events have been the topic of a number of paleontological debates that cannot be resolved without a reliable regional and global chronostratigraphic framework. Of principle interest are investigations of (1) the likelihood that ice sheet growth caused positive shifts in the marine oxygen isotope record and widespread unconformities in continental margin stratigraphic sequences during the mid-Campanian, late Campanian and early Maastrichtian (Miller and others, 1999, 2005; Jarvis and others, 2002; Huber and others, 2002); (2) whether global warming (inferred from oxygen isotopes) and poleward migration of thermophilic planktonic foraminifera during the latest Maastrichtian were synchronous with the onset of Deccan Trap volcanism, as has been reported by various authors (e.g., Huber, 1990; Huber and Watkins, 1992; Barrera and Savin, 1999; Olsson and others, 2001); (3) the nature of the "mid-Maastrichtian Event," for which global extinction among deep-sea inoceramid bivalves has been related to a change in deep-ocean circulation, as evidenced by a negative excursion in global deep-sea benthic carbon isotope values and a positive shift in oxygen isotope values (MacLeod, 1994; MacLeod and Huber, 1996; MacLeod and others, 2000; Frank and Arthur, 1999; Frank and others, 2005); and (4) extinction patterns of planktonic foraminifera below and across the Cretaceous-Paleogene mass extinction event (e.g., Keller, 1988, 2004; Keller and others, 1993; Abramovich and others, 1998; Norris and others, 1998; Arenillas and others, 2000; Arz and others, 2000, 2001; Huber and others, 2002; Molina and others, 2005; MacLeod and others, 2007).

Late Campanian-Maastrichtian sediments drilled on the Blake Nose, in the subtropical North Atlantic Ocean (Fig. 1), have figured prominently in these debates because of the unusually good preservation of calcareous microfossils and relatively complete composite core recovery for a region and range of depths otherwise lacking good Campanian-Maastrichtian data. Deep Sea Drilling Project (DSDP) Hole 390A (Leg 44; Benson and others, 1978) and Ocean Drilling Program (ODP) Sites 1049, 1050 and 1052 (Leg 171B; Norris and others, 1999) were drilled along a 50-km depth transect from 2700 to 1300 m water depth at the edge of the Blake Nose escarpment (Fig. 1). Paleolatitude of the sites is estimated as 25°N (Ogg and Bardot, 2001). A seismic reflection profile across this transect reveals a shallowly buried Aptian-Eocene sequence of pelagic ooze and chalk that gently slopes and gradually thins eastward to the Blake Escarpment (Norris and others, 1998, p. 353, Fig. 3). The Campanian-Maastrichtian interval is thickest at Site 1052, which recovered 172 m of hemipelagic chalk, and is thinnest at Site 1049 and Hole 390A, which recovered about 20 m of pelagic chalk. Although slump features are apparent at several levels of all three sites (Norris and others, 1998), no evidence for stratigraphic repetition has been presented (MacLeod and others, 2003).

Detailed investigations of faunal and stable isotopic investigations associated with the "mid-Maastrichtian Event" (*sensu* Frank and others, 2005) have been undertaken on samples from Hole 390A (MacLeod and others, 2000; Friedrich and others, 2004), and the site was resampled as Site 1049 of ODP Leg 171B. Isotopic trends and their relationship to Maastrichtian North Atlantic paleoceanography and foraminiferal paleobiology were examined at Sites 1050 and 1052 (MacLeod and others, 2005; Isaza-Londoño and others, 2006). Campanian-Maastrichtian studies of the Leg 171B Blake Nose drill sites also include examination of relative abundance changes among planktonic foraminifera and calcareous nannofossils below and across the Cretaceous-Paleogene boundary (Norris and others, 1999; Huber and others, 2002; Self-Trail, 2001, 2002; Watkins and Self-Trail, 2005); strontium isotope evidence for slope failure, sediment reworking and ocean chemistry related to the boundary (MacLeod and others,

[1] Department of Paleobiology, MRC-121, Smithsonian Museum of Natural History, Washington, DC 20013-7012
[2] Department of Geological Sciences, University of Missouri-Columbia, Columbia, MO 65211
[3] All-Russian Geological Institute (VSEGEI), Sredny pr., 74, St.-Petersburg, 199106 Russia
[4] Correspondence author. E-mail: huberb@si.edu

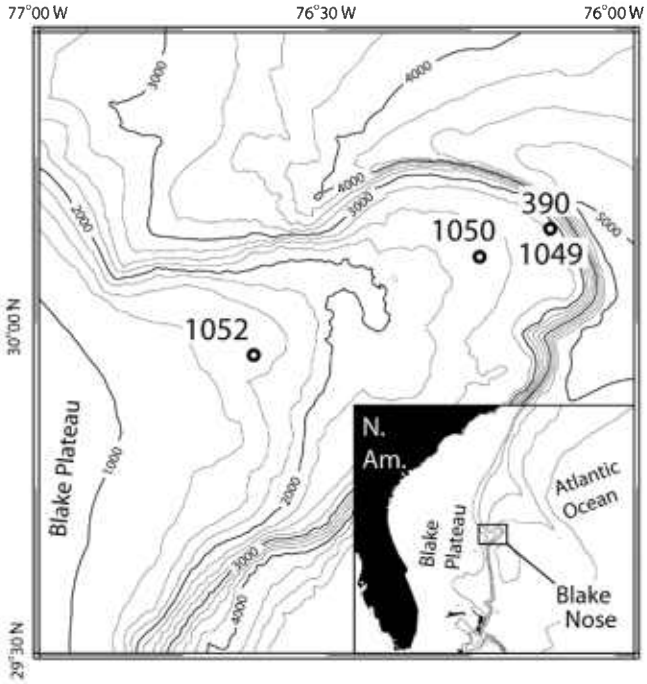

FIGURE 1. Location of DSDP Hole 390A and ODP Sites 1049, 1050 and 1052 on the Blake Nose and relative to the southeast coast of North America (inset). Depth in meters.

2001a; MacLeod and others, 2003); long- and short-term variations in the oxygen and carbon isotopic record (MacLeod and others, 2000, 2005; MacLeod and Huber, 2001; Wilf and others, 2003), and the effects of Milankovitch forcing on sedimentation and foraminiferal distributions during the mid-Maastrichtian (MacLeod and others, 2001b). Collectively, these studies span a range of important paleoceanographic and paleoclimatological topics, but they have used a variety of age models that complicate integration of the results and comparison of Blake Nose patterns to events documented in other regions.

The objective of this study is to develop age-depth models for the Campanian-Maastrichtian intervals at each of the Blake Nose sites using the best available planktonic foraminiferal, calcareous nannofossil and paleomagnetic datum events calibrated with a current geological time scale (Gradstein and others, 2004). Better age models enable a more reliable calculation of sedimentation rates, determination of the distribution and duration of hiatuses, and estimation of ages for first and last occurrence datums of previously uncalibrated planktonic foraminiferal and calcareous nannofossil species. Most importantly, establishment of the age-depth relationships for each of the Blake Nose sites enables examination of the degree to which biotic and paleoceanographic events observed on the Blake Nose are synchronous across the depth transect and with events observed at other localities worldwide.

MATERIAL AND METHODS

Planktonic foraminifera are abundant, and the assemblages are diverse and moderately to very well preserved at each of the Blake Nose sites (Norris and others, 1998). Sampling resolution from Leg 171B sites varies depending on proximity to bio- and lithostratigraphic boundaries and thickness of the Campanian-Maastrichtian interval. A total of 40 samples between 132.25 and 112.97 meters below seafloor (mbsf) were studied from Hole 1049C with an average sample spacing of less than 0.5 m; 53 samples between 484.56 and 405.92 mbsf were studied from Hole 1050C with an average sample spacing of 1.5 m; and 85 samples between 475.45 and 302.17 mbsf were studied from Hole 1052E with an average sample spacing of 2.0 m. For Hole 390A samples from the study of MacLeod and others (2000), which generally had 0.75-m sample spacing, were analyzed and supplemented with additional samples to improve biostratigraphic resolution and to identify datum events that were not recognized in the MacLeod and others (2000) study.

Most nannofossil datums reported are from published sources. The ages and depths used are cited in Tables 1–5. Smear slides were prepared during the present study for select Maastrichtian samples from DSDP Hole 390A and ODP Hole 1049C in an effort to determine the stratigraphic distribution of several calcareous nannofossil zonal marker taxa that are included in Tables 2 and 3.

Paleomagnetic chron assignments for the Leg 171B drill sites are based on the magnetic polarity data of Ogg and Bardot (2001), which include shipboard measurement of natural remnant magnetization of continuous half-core sections yielding a sample resolution of about 5 cm. These data were supplemented by shore-based progressive demagnetization of about two discrete samples per core-section (about 0.75 m apart). As noted in Ogg and Bardot (2001), many of the polarity chron boundaries in the Campanian-Maastrichtian cores were indeterminate because of stratigraphic discontinuities, poor paleomagnetic characteristics and synsedimentary slumping and/or drilling-induced disruption. As a result, only chron boundaries deemed to be reliably identified and stratigraphically well located were included in the age models.

Age-depth models were created using the *CHRONOS* ADP application with an interactive line of correlation (LOC) drawn through the most reliable stratigraphic event data points (see http://www.chronos.org). Stratigraphic uncertainty is plotted as vertical bars to show the thickness between samples containing the datum marker and the next sample below or above where the datum marker is absent. Table 1 lists the bioevents, associated biozones and datum ages used in the age models. Bioevent ages originally reported relative to previous time scales (e.g., Gradstein and others, 1994; Cande and Kent, 1995; Hardenbol and others, 1998, Chart 5) were converted by J. Ogg, (pers. comm., 2007) to the Geologic Time Scale 2004 (GTS2004; Gradstein and others, 2004) by maintaining the same relative position in the polarity chrons and adjusting to 0.01-m.y. precision. Sources for bioevent depths are cited in Tables 2–5. In the present study, we distinguish between lowest (LO) and highest (HO) occurrences of marker species, which are used to define biozone boundaries within the sections, and first-appearance (FAD) and last-appearance (LAD) datums, which are used to define globally the temporal limits of a bioevent.

As an independent check on the accuracy of the age model, we used the interpreted age-depth relationship from age

TABLE 1. Planktonic foraminiferal (F) and calcareous nannofossil (N) datums used in late Campanian-Maastrichtian age models for the Blake Nose drill sites. Sources for ages and comments on datums are shown.

Fossil Group	Datum Event	Zone (Base)	Datum	Cande & Kent (1995) Age (Ma)	SEPM 1998[6]	Gradstein and others (2004); This study Age (Ma)[7]	Comment
N	b *Micula prinsii*	CC26b[1]	bMp	66.00[5]	66.15	66.79	Henriksson (1993) identified the LO of *M. prinsii* in lower Chron C29r at DSDP sites in the Atlantic and Pacific Oceans. Averaging its distribution within this chron interval for sites with moderate abundance of this species yields a mean age of 65.79 Ma.
N	b *Ceratolithoides kamptneri*	CC26a[1]	bCk	67.20[1]		[67.44]	Perch-Nielsen (1985) noted that *C. kamptneri* can be used as a proximal marker for the base of Zone CC26.
N	b *Nephrolithus frequens*	CC26a[1]	bNf	67.20[5]	68.15	67.44	Pospichal and Wise (1990) identified the LO of *N. frequens* at near same level as *Reinhardtites levis* in middle Chron C31r at Maud Rise and note an ~1 m.y. younger appearance at low latitudes within Chron C31n.
F	b *Pseudoguembelina hariaensis*	*Psuedoguembelina hariaensis*[2]	bPh	66.40[2]	66.54	[66.78]	Li and Keller (1998) identified the LO of *P. hariaensis* in middle Chron C30n at DSDP Site 525A in the mid-latitude South Atlantic.
N	b *Micula murus*	CC25c[1]	bMm	68.50[1]	68.66	68.51	Monechi and Thierstein (1985) placed at base of Chron C30n in the Bottaccione section (~67.70 Ma). Erba and others (1995) assigned this to upper Chron C31r, which is the preferred age used here.
F	b *Abathomphalus mayaroensis*	*Abathomphalus mayaroensis*	bAm	68.25[2]	68.66	[68.72]	Recorded at base of Chron C31n by Monechi and Thierstein (1985) in Bottaccione section, which is where it first occurs in the present study; recorded in lower to middle Chron C31r at ODP Sites 689 and 690 (Maud Rise, southern South Atlantic; Huber, 1990) and Hole 525A mid-latitude South Atlantic; Li and Keller, 1998).
N	b *Lithraphidites quadratus*	CC25b[1]/UC20[3]	bLq	67.50	68.56	68.70	Monechi and Thierstein (1985) assigned to lowermost Chron C31n in the Bottaccione section, or ~68.70 Ma.
N	t *Reinhardtites levis*	CC25a[1]/UC19[3]	tRl	69.20[5]	69.42	69.44	Pospichal and Wise (1990) noted latitudinal diachroneity in this extinction, with low latitude HO at the base of Chron C30n and high latitude HO in middle Chron C31r. However, Erba and others (1995) record this HO just above the LO of *R. fructicosa*, which is the level used here. Bralower and others (1995) do not differentiate *R. levis* from *R. anthophorus* because of difficulty separating morphologies with even minor diagenesis.
F	b *Racemiguembelina fructicosa*	*Racemiguembelina fructicosa*	bRf	69.60[5]	69.44	69.62	At low latitudes, Premoli Silva and Sliter (1994) and Robaszynski and Caron (1995) correlate LO in Tunisia with the upper third of Chron C31r. Latitudinal diachroneity is demonstrated by LO in Chron C31n at DSDP Site 525 (Li and Keller, 1998).
N	t *Quadrum trifidum*		tQt	71.30[5]	70.55	69.85	According to J. Ogg (commun., 2007) datum occurs ~0.75 m.y. above Tercis GSSP base of Maastrichtian (used here).
N	t *Tranolithus orionatus*	UC18[3]	tTo	69.60[5]	69.82	[70.60]	Leg 207 Initial Reports volume (Shipboard Scientific Party, 2004) uses this HO for base of CC24 rather than *T. phacelosus*, but most workers consider it difficult to distinguish *T. orionatus* from *T. phacelosus*, and consider the latter species as the senior synonym (J. Self-Trail, commun., 2007).
F	b *Pseudoguembelina palpebra*	*Pseudoguembelina palpebra*	bPp			71.64	At Blake Nose (this study) the LO of *P. palpebra* occurs just above both Chron C32n.1r and the FAD of the calcareous nannofossil *T. phacelosus*.
N	t *Tranolithus phacelosus*	CC24[4]	tTp	71.60[5]	71.30	71.80	Erba and others (1995) correlate with the base of Chron C32n.1, which is the age used here.
F	b *Gansserina gansseri*	*Gansserina gansseri*	bGg	72.80[5]	72.84	72.35	Premoli Silva and Sliter (1994) place at about 40% above the base of Chron C32n.n2. This species is not a reliable datum at Blake Nose because of its sporadic and rare occurrence in the core samples.

TABLE 1. Continued.

Fossil Group	Datum Event	Zone (Base)	Datum	Cande & Kent (1995) Age (Ma)	SEPM 1998[6]	Gradstein and others (2004); This study Age (Ma)[7]	Comment
F	b *Planoglobulina acervulinoides*		bPa		72.84	72.35	Premoli Silva and Sliter (1994) place at same level as LO of *G. gansseri*, about 40% above the base of Chron C32n.n2. At the Blake Nose sites the LO of *P. acervulinoides* consistently occurs at or just above the LO of *R. fructicosa*. This discrepancy may result from differing taxonomic concepts of this species.
F	b *Globotruncana aegyptiaca*	*Globotruncana aegyptiaca*	bGa		74.08	73.27	Premoli Silva and Sliter (1994) place at about 50% above the base of Chron C32r.r2. This is an unreliable datum at Blake Nose because of the sporadic occurrence of the biomarker.
F	b *Pseudoguembelina excolata*		bPe		74.08	73.27	Premoli Silva and Sliter (1994) report at same level (mid-C32r.r2) as the LO of *G. aegyptiaca*.
F	b *Pseudotextularia elegans*		bPel		75.25	[75.07]	SEPM'98 places at same level (C33n.85) as HO of *R. calcarata*, which is the basis for the age estimate used here.
N	t *Aspidolithus parcus*	UC17[3]	tAp	74.60[5]	74.47	[73.90]	Monechi and Thierstein (1985) place at Chron C33r.60 in the Bottaccione section, but Erba and others (1995) correlate with the base of Chron C32r.2r, which is followed here. Gradstein and others (2004) use 75.20 Ma as the LAD for this species. Also placed in genus *Broinsonia*.
F	t *Radotruncana calcarata*	*Globotruncanella. havanensis*	tRc	75.20[2]	75.77	[75.07]	Assigned to polarity Chron C33n.92 based on Bottaccione section (Premoli Silva and Sliter, 1994). Gradstein and others (2004) use 75.57 Ma as datum age. Previously has been assigned to *Globotruncanita*.
N	t *Eifellithus eximius*	CC23[4]/UC16[3]	tEe	75.30[5]	75.33	[75.31]	Monechi and Thierstein (1985) record in ~Chron C33n.50 in Bottaccione section, whereas Erba and others correlate with ~Chron C33n.80, which is used here. Gradstein and others (2004) use 75.72 Ma as datum age.
F	b *Radotruncana calcarata*	*Radotruncana calcarata*	bRc	76.40[2]	76.20	[75.57]	Assigned to Chron C33n.76 based on Bottaccione section (Premoli Silva and Sliter, 1994). Gradstein and others (2004) use 76.18 Ma as datum age. Previously has been assigned to *Globotruncanita*.
N	b *Quadrum trifidum*	CC22[4]	bQt	76.00[5]	76.15	76.29	In the Bottaccione section, Premoli Silva and Sliter correlate with just above the LO of *R. calcarata*, but Erba and others record lower, at about Chron C33.65, which is the age estimate used here. Gradstein and others (2004) use 76.38 Ma as datum age. Also known as *Uniplanarius trifidum*.
N	b *Quadrum sissingh*	CC21[4]	bQs	77.00[5]	77.15	77.10	Erba and others (1995) correlate with ~Chron C33n.45, which is the estimate used here. Gradstein and others (2004) use 77.38 Ma as datum age. Also known as *Uniplanarius sissinghii*.
F	b *Globotruncana ventricosa*	*Globotruncana ventricosa*	bGv		77.58	79.54	In the Bottaccione section, Premoli Silva and Sliter (1994) record at base of Chron C33n. Gradstein and others (2004) place in upper Chron C33r with an assigned age of 79.92 Ma.

[1]Self-Trail, 2001
[2]Robaszynski and Caron, 1995
[3]Burnett, 1998
[4]Sissingh (1977) and Perch Nielsen (1985)
[5]Erba and others, 1995
[6]SEPM 1998 refers to Chart 5 in de Graciansky and others, 1998
[7]Age values presented in brackets are recalibrated to the Gradstein and others (2004) time scale.

models for each site to generate an estimated age for each Campanian-Maastrichtian Blake Nose sample for which $^{87}Sr/^{86}Sr$ data are available (MacLeod and others, 2001a; MacLeod and others, 2003). These ages and ratios are then plotted against the $^{87}Sr/^{86}Sr$ seawater curve of McArthur and Howarth (2004). Like the age model, this Sr-curve is calibrated to the time scale of Gradstein and others (2004). However, because of a consistent offset in similarly aged samples observed between samples from a number of sites analyzed at the University of North Carolina and those used to define the mean Late Cretaceous seawater strontium curve, the reference curve was shifted by 0.000020 toward higher values (MacLeod and others, 2003).

BIOZONATION

The planktonic foraminiferal zonal scheme outlined below is based on the standard tropical/subtropical scheme of Robaszynski and Caron (1995), which was established for the families Globotruncanidae and Heterohelicidae based on observations from Cretaceous sections in the Mediterranean region. This scheme has been modified to improve reliability of correlation among the Blake Nose drill sites by including recognition of a new *Pseudoguembelina palpebra* Partial-range Zone between the *Globotruncanella havanensis* and *Racemiguembelina fructicosa* Zones. Other modifications and refinements are noted in the remarks subsection of the zonal descriptions below. Ages of the zonal marker datums and sources for those ages are cited in Table 1. Biostratigraphic subdivisions of each Blake Nose drill site are correlated relative to the drill site magnetostratigraphy and the Robaszynski and Caron (1995) biozonation in Figures 2–5. Datums used to define the calcareous nannofossil tropical/subtropical biozonations of Sissingh (1977) and Perch-Nielsen (1985), as adopted by Self-Trail (2002) and identified in this study, are listed in Table 1 and presented in Figures 2–5.

Globotruncana ventricosa Partial-range Zone (=*Globotruncana ventricosa* Interval Zone of Robaszynski and Caron, 1995)

Definition. Biostratigraphic interval from the lowest-occurrence of the nominate species to the lowest occurrence of *Radotruncana calcarata.*

Magnetochronologic calibration. Premoli Silva and Sliter (1994) record the LO at the same level as the base of Chron C33n in the Bottaccione section.

Age Estimates. Base 79.54 Ma, top 75.57 Ma.

Remarks. Although the zonal marker was found only in one sample, the zonal interval is assigned to all of Core 1050C-19R based on the presence of *Globotruncanita subspinosa*, *G. atlantica*, *G. elevata*, *Contusotruncana patelliformis* and *C. plummerae* and the absence of *Radotruncana calcarata.* The lower part of this zone at Site 1050 is truncated by an unconformity. This zone is absent from the other Blake Nose drill sites.

In addition to the species listed above, characteristic globotruncanids within this zone include *Globotruncana arca*, *G. bulloides*, *G. hilli*, *G. linneiana*, *Globotruncanita stuartiformis*, and *Contusotruncana fornicata.* Heterohelicid species include *Heterohelix globulosa* and *Pseudotextularia nuttalli.*

Radotruncana calcarata Taxon-range Zone (=*Globotruncana calcarata* Total Range Zone of Robaszynski and Caron, 1995)

Definition. Biostratigraphic interval comprising the total range of the nominate species (Fig. 2).

Magnetochronologic calibration. Based on the study of Premoli Silva and Sliter (1994), the LO and HO of *R. calcarata* are estimated at 76% and 92%, respectively, above the base of Chron C33n in the Bottaccione section. At ODP Site 1050 the LO of *R. calcarata* correlates with a normal polarity zone assigned to C33n (Fig. 4).

Age Estimates. Base 75.57 Ma, top 75.07 Ma.

Remarks. The nominate species is a rare but conspicuous element found throughout this zone. The stratigraphic range of *R. calcarata* in the Bottaccione section may be underestimated because of difficulty in making unambiguous identification of specimens with spines in thin section (Premoli Silva and Sliter, 1994). Thus, ages for its FAD and LAD may be underestimated.

Characteristic globotruncanid species found in this zone include *Globotruncana arca*, *G. angulata*, *G. atlantica*, *G. bulloides*, *G. insignis*, *G. orientalis*, *Globotruncanita stuartiformis*, *Contusotruncana fornicata* and *C. patelliformis.* Characteristic heterohelicid species include *Heterohelix globulosa* and *Pseudotextularia nuttalli.*

LOs observed within this zone include *Planoglobulina manuelensis*, *P. riograndensis*, *Pseudoguembelina costulata*, *Gublerina acuta* and *Globotruncanella havanensis.*

Globotruncanella havanensis Partial-range Zone (=*Globotruncanella havanensis* Interval and Partial Range Zone of Robaszynski and Caron, 1995)

Definition. Biostratigraphic interval containing the partial range of the nominate taxon from the HO of *Radotruncana calcarata* to the LO of *Pseudoguembelina palpebra* (Fig. 2).

Magnetochronologic calibration. See above for base and below for top of zone.

Age Estimates. Base 75.07 Ma, top 71.64 Ma.

Remarks. The nominate species is relatively rare within this zone, whereas globotruncanids including *Globotruncana arca*, *G. linneiana*, *G. bulloides*, *Contusotruncana fornicata* and *Globotruncanita stuartiformis* are quite common. Among the heterohelicids, *Heterohelix globulosa* is common and *Pseudotextularia nuttalli*, *Laeviheterohelix glabrans* and *Planoglobulina riograndensis* are present but relatively rare.

Numerous lowest occurrences are recorded within this zone. Species with LOs near the base of the zone include *Pseudoguembelina excolata*, *Globotruncanita stuarti* and

TABLE 2. Biostratigraphic datums used to define the age-depth curve for ODP Hole 1049C.

Datum type	Event	Plot-code	Young age (Ma)	Top depth (mbsf)	Bottom depth (mbsf)
KPB	K/P boundary[1]	KPB	65.50	113.07	113.07
M	bChron C29r[2]	bC29r	65.86	113.89	115.24
F	b *G.aegyptiaca*[3]	bGa	73.27	120.18	120.68
N	b *M. prinsii*[4]	bMp	65.81	123.61	125.08
F	b *P. hariaensis*[3]	bPh	66.78	123.61	124.10
N	b *C. kamptneri*[4]	bCk	67.44	125.08	125.56
N	b *M. murus*[4]	bMm	68.51	125.08	125.56
F	b *A. mayaroensis*[3]	bAm	68.72	125.08	125.56
F	b *R. fructicosa*[3]	bRf	69.62	125.56	126.54
F	b *P. acervulinoides*[3]	bPa	72.35	125.56	126.54
F	b *P. elegans*[3]	bPel	75.07	125.56	126.54
F	b *G. gansseri*[3]	bGg	72.35	128.49	129.47
F	b *P. excolata*[3]	bPex	73.27	129.69	130.20
F	t *R. calcarata*[3]	tRc	75.07	130.20	130.70
N	t *E. eximius*[5]	tEe	75.31	130.70	131.97
N	b *Q. trifidum*[5]	bQt	76.29	130.70	131.97
F	b *R. calcarata*[3]	bRc	75.57	132.33	132.40

[1]Norris and others, 1998
[2]Ogg and Bardot, 2001
[3]This study
[4]Self-Trail, 2002
[5]Watkins *in* Norris and others, 1998

Rugoglobigerina hexacamerata; LOs in the middle of the zone include *Globotruncanella petaloidea* and *Gublerina robusta*.

Pseudoguembelina palpebra Partial-range Zone (defined herein; different denotation than *Pseudoguembelina palpebra* Zone of Li and Keller, 1998)

Definition. Biostratigraphic interval from the LO of *Pseudoguembelina palpebra* to the LO of *Racemiguembelina fructicosa*.

Magnetochronologic calibration. At Site 1050, the LO of *P. palpebra* occurs 21 cm above the midpoint depth of Chron C32n.1r (this study). The LO of *R. fructicosa* correlates with the upper third of Chron C31r in southern Europe (Premoli Silva and Sliter, 1994; Robaszynski and Caron, 1995) and in the subtropical North Atlantic Ocean (this study). The LO of *R. fructicosa* within the middle of Chron C31n in the mid-latitude South Atlantic Ocean (Li and Keller, 1998) may be the result of poleward diachroneity in its distribution.

Age Estimates. Base 71.64 Ma, top 69.62 Ma.

Remarks. The LO of the nominate taxon is determined by the appearance of a finely costate biserial heterohelicid that has a rapid chamber-size increase in the early ontogeny and the distinct presence of at least one supplementary aperture. These early forms strongly resemble the holotype of *Pseudoguembelina polypleura* Masters, 1976, which is considered a junior synonym of *P. palpebra* by most authors (e.g., see Nederbragt, 1991). Later forms tend to show increased pinching of the final chambers, greater inflation of the prepenultimate chambers, a more coarsely costate test, and earlier ontogenetic appearance of the supplementary apertures than early forms. However, the change is gradual through the section, with a range of morphologies possible in any given sample.

The LO of *P. palpebra* is consistently found in low to moderate abundance between the HO of *R. calcarata* and the LO of *R. fructicosa* at all of the Blake Nose drill sites and is recorded just above the LO of *Gansserina gansseri* in Hole 1049C. Because *G. gansseri* has a spotty distribution in the Blake Nose samples and is very rare when it is found, the LO of *P. palpebra* is considered a more reliable biomarker than the LO of *G. gansseri* for correlation within the uppermost Campanian interval. The FAD of *P. palpebra* is estimated as 71.64 Ma based on ages averaged

TABLE 3. Biostratigraphic datums used to define the age-depth curve for DSDP Hole 390A.

Datum type	Event	Plot-code	Young age (Ma)	Top depth (mbsf)	Bottom depth (mbsf)
KPB	K/P boundary	KPB	65.50	111.87	112.20
F	b *P. hariaensis*	bPh	66.78	125.01	125.77
N	b *C. kamptneri*	bCk	67.44	125.77	125.87
N	b *M. murus*	bMm	68.51	125.77	125.87
F	b *A. mayaroensis*	bAm	68.80	125.77	125.87
F	b *R. fructicosa*	bRf	69.56	126.36	126.85
F	t *R. calcarata*	tRc	75.07	139.32	139.48
F	b *R. calcarata*	bRc	75.57	140.14	140.31
F	b *G.aegyptiaca*	bGa	73.27	124.37	125.01
F	b *P. elegans*	bPel	75.07	125.77	126.36

TABLE 4. Biostratigraphic datums used to define the age-depth curve for ODP Hole 1050C.

Datum type	Event	Plot-code	Young age (Ma)	Top depth (mbsf)	Bottom depth (mbsf)
F	K/P boundary[1]	KPB	65.50	405.97	405.97
N	b *M. prinsii*[2]	bMp	65.81	427.00	428.50
F	b *P. hariaensis*[3]	bPh	66.78	427.92	428.93
N	b *C. kamptneri*[2]	bCk	67.44	427.00	428.50
N	b *M. murus*[2]	bMm	68.51	446.30	448.20
N	b *L. quadratus*[2]	bLq	68.70	450.50	452.20
F	b *A. mayaroensis*[3]	bAm	68.72	451.51	451.82
M	bC31n[4]	bC31n	68.79	452.47	453.03
F	b *R. fructicosa*[3]	bRf	69.62	456.29	462.17
N	t *R. levis*[2]	tRl	69.44	475.20	478.20
M	bC32n.1r[4]	bC32n.1r	71.47	476.46	477.56
N	t *T. phacelosus*[2]	tTp	71.80	475.20	478.20
F	b *G. gansseri*[3]	bGg	72.35	473.70	474.30
F	b *P. acervulinoides*[3]	bPa	72.35	462.17	463.55
F	b *G. aegyptiaca*[3]	bGa	73.27	476.55	478.15
F	b *P. excolata*[3]	bPe	73.27	476.55	478.15
F	b *P. elegans*[3]	bPel	75.07	467.20	468.70
F	t *R. calcarata*[3]	tRc	75.07	478.15	478.86
N	t *A. parcus*[4]	tAp	74.65	478.20	478.90
F	b *R. calcarata*[3]	bRc	75.57	478.86	481.69
N	t *E. eximius*[5]	tEe	75.31	478.90	482.30
N	b *Q. sissingh*[5]	bQs	77.10	491.30	491.40
F	b *G. ventricosa*[5]	bGv	79.54	484.56	491.02

[1]Norris and others, 1998
[2]Self-Trail, 2002
[3]This study
[4]Ogg and Bardot, 2001
[5]Watkins *in* Norris and others, 1998

from its LOs at ODP Sites 1049 and 1050, which differ by only 0.21 m.y. (Table 7). The age of the lowest occurrence of *P. palpebra* in Hole 1052E is not calculated because of an unconformity separating upper Campanian from lower Cenomanian sediments.

Globotruncanid assemblages in the *P. palpebra* Zone are very similar to those found in the underlying *G. havanensis* Zone. *Globotruncana arca*, *G. bulloides*, *G. linneiana* and *Globotruncanita stuartiformis* are most abundant and *G. hilli* and *C. patelliformis* increase in abundance up section. Heterohelicids are dominated by *Heterohelix globulosa* and *Pseudotextularia nuttalli*. *Pseudoguembelina palpebra*, *P. costulata*, *Heterohelix navarroensis*, *H. labellosa*, *Gublerina acuta*, *Planoglobulina manuelensis*, and *P. riograndensis* occur consistently in low to moderate abundance.

TABLE 5. Biostratigraphic datums used to define the age-depth curve for ODP Hole 1052E.

Group	Event	Plot Code	Young Age (Ma)	Top depth (mbsf)	Bottom depth (mbsf)
KPB	k/t boundary[1]	KPB	65.50	302.18	302.18
M	b C29r[2]	b29r	65.86	302.79	309.70
F	b *M. prinsii*[3]	bMp	65.81	324.60	326.00
F	b *P. hariaensis*[4]	bPh	66.78	328.88	330.32
M	base C30n[2]	b30n	67.70	335.62	338.71
M	base C30r[2]	b30r	67.87	343.68	349.30
N	b *C. kamptneri*[3]	bCk	67.44	351.80	352.90
N	b *M. murus*[3]	bMm	68.51	367.90	377.10
F	b *A. mayaroensis*[4]	bAm	68.72	379.01	380.28
N	b *L. quadratus*[3]	bLq	68.70	385.00	386.70
M	b C31n[2]	bC31n	68.79	386.26	386.73
N	t *R. levis*[3]	tRl	69.44	389.92	394.28
F	b *R. fructicosa*[4]	bRf	69.62	400.12	411.99
M	b C31r[2]	bC31r	70.96	468.35	478.35
F	b *P. acervulinoides*[4]	bPa	72.35	386.67	394.26
F	b *G. aegyptiaca*[4]	bGa	72.35	414.52	418.50
F	b *G. gansseri*[4]	bGg	72.35	473.70	474.30
N	t *T. phacelosus*[5]	tTp	71.80	474.00	474.40
F	b *P. elegans*[4]	bPel	75.07	423.27	424.22

[1]Norris and others, 1998
[2]Ogg and Bardot, 2001
[3]Self-Trail, 2002
[4]This study
[5]Watkins *in* Norris and others, 1998

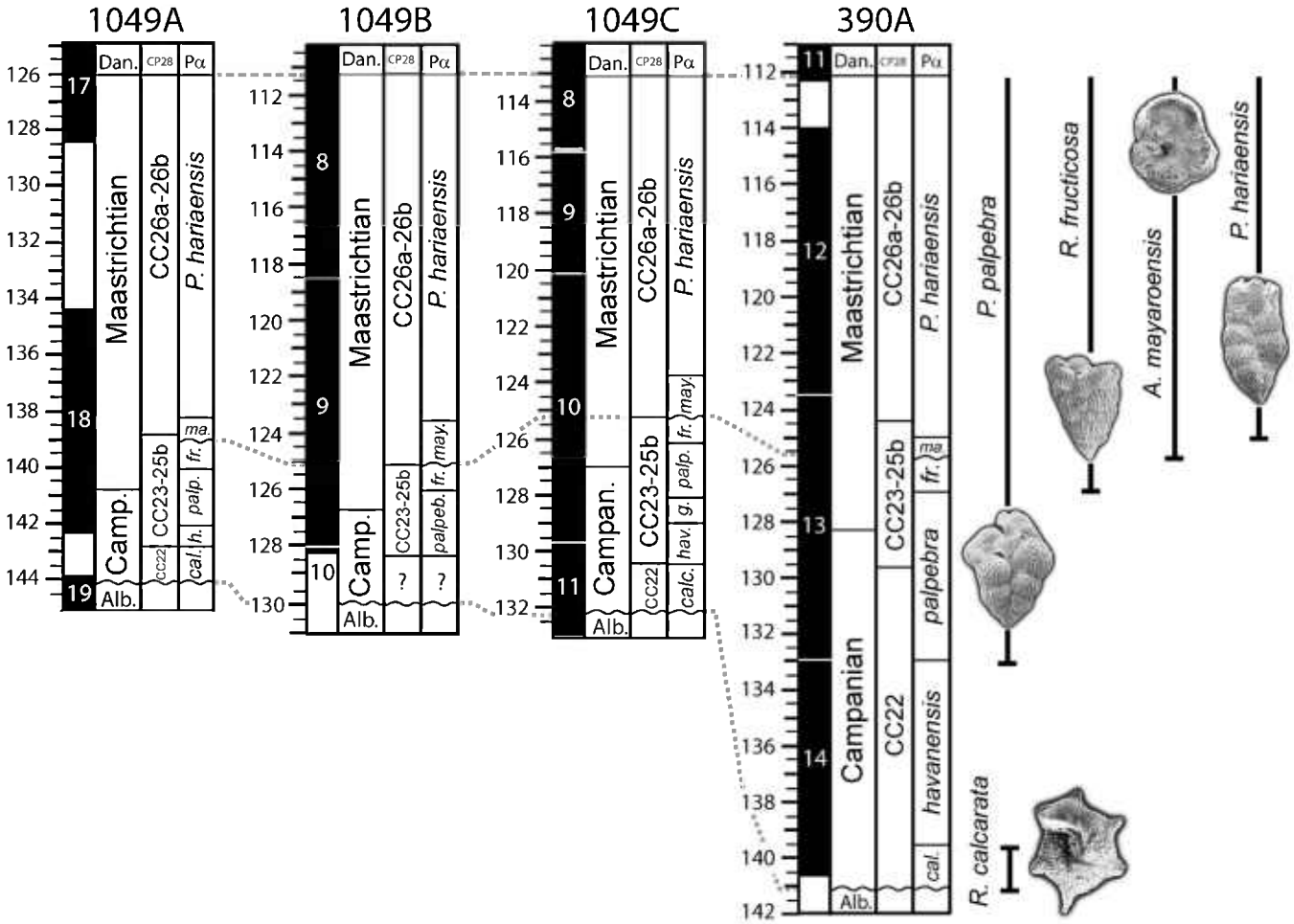

FIGURE 2. Comparison of meters-below-seafloor depths for planktonic foraminiferal and calcareous nannofossil biozones in ODP Site 1049 and DSDP Hole 390A showing core recovery in each hole (black = recovered intervals). Dashed line correlates the Cretaceous/Paleogene boundary, and dotted lines correlate major unconformities at the base of the *Abathomphalus mayaroensis* Biozone and *Radotruncana calcarata* Biozone. Planktonic foraminiferal zonal datums and SEM images are shown to the right. See Table 1 for full spelling and definitions of biozones.

Lowest occurrences within the lower part of this zone include *Pseudoguembelina kempensis* and *Racemiguembelina powelli*. LOs in the upper part of the zone include *Planoglobulina multicamerata*, *Pseudotextularia intermedia*, *P. brazoensis* and *Contusotruncana contusa*.

Racemiguembelina fructicosa Partial-range Zone (base different, top same as *Racemiguembelina fructicosa* Partial-range Zone of Robaszynski and Caron, 1995)

Definition. Biostratigraphic interval from the LO of *Racemiguembelina fructicosa* to the LO of *Abathomphalus mayaroensis*.

Magnetochronologic calibration. See above for LO of *R. fructicosa*. In the Italian Bottaccione section, the LO of *A. mayaroensis* correlates with the base of Chron C31n (Premoli Silva and Sliter, 1994), whereas it has been reported in lower to middle Chron C31r in the South Atlantic Ocean (Huber, 1990; Li and Keller, 1998).

Age Estimates. Base 69.62 Ma, top 68.72 Ma.

Remarks. The LO of *R. fructicosa* is differentiated from its ancestor, *R. powelli*, by having smaller, more numerous multiserial chambers that form a more circular test outline in top view and are connected by a sieve plate (Nederbragt, 1991). However, presence of intermediate forms may cause some uncertainty in identifying this datum. The nominate species is rare in the lower part of the zone and becomes increasingly abundant in the upper part.

Characteristic globotruncanid species include *Globotruncana arca*, *G. conica*, *G. hilli*, *Gobotruncanita stuartiformis* and *Contusotruncana contusa*. *Globotruncana bulloides* becomes very rare in the upper part of the zone. Heterohelicids are dominated by *Heterohelix globulosa*, *H. striata* and *H. navarroensis*, whereas *Heterohelix labellosa*, *Pseudotextularia elegans*, *Planoglobulina multicamerata* and *Pseudoguembelina palpebra* occur consistently in low to moderate abundance. *Planoglobulina manuelensis* becomes less abundant in the upper part of this zone.

LOs within this zone include *Heterohelix semicostata*, *Planoglobulina acervulinoides* and *Rugoglobigerina rotundata*. The HO of *Contusotruncana fornicata* is recorded in the middle of this zone.

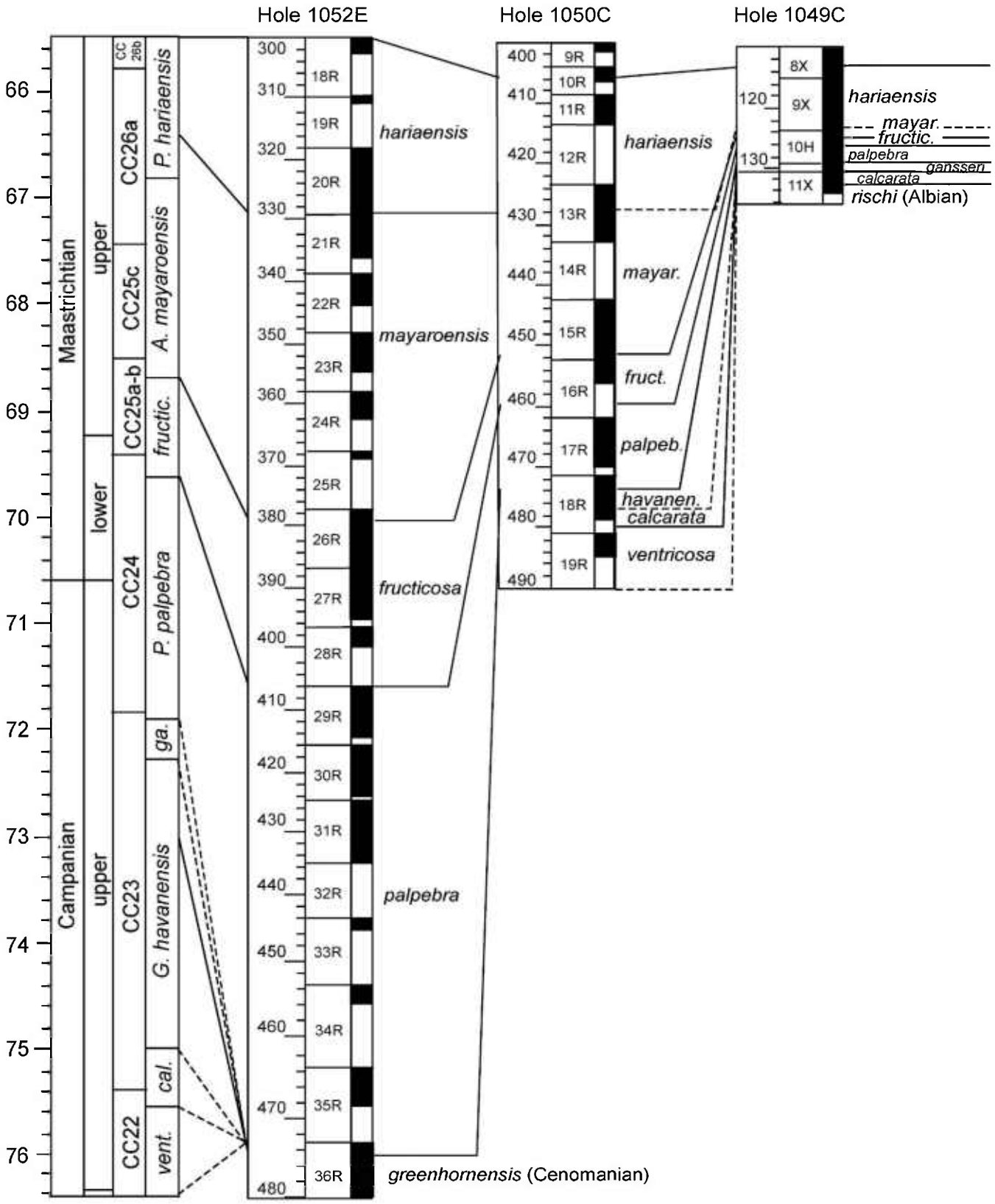

FIGURE 3. Correlation of upper Campanian-Maastrichtian meters-below-seafloor depths, core number, amount of recovered core (white = coring gap), and planktonic foraminiferal biozones for the Leg 171B drill sites. Dashed lines indicate that the zonal boundary occurs at an unconformity. See text for complete spelling and definitions of planktonic foraminiferal biozones.

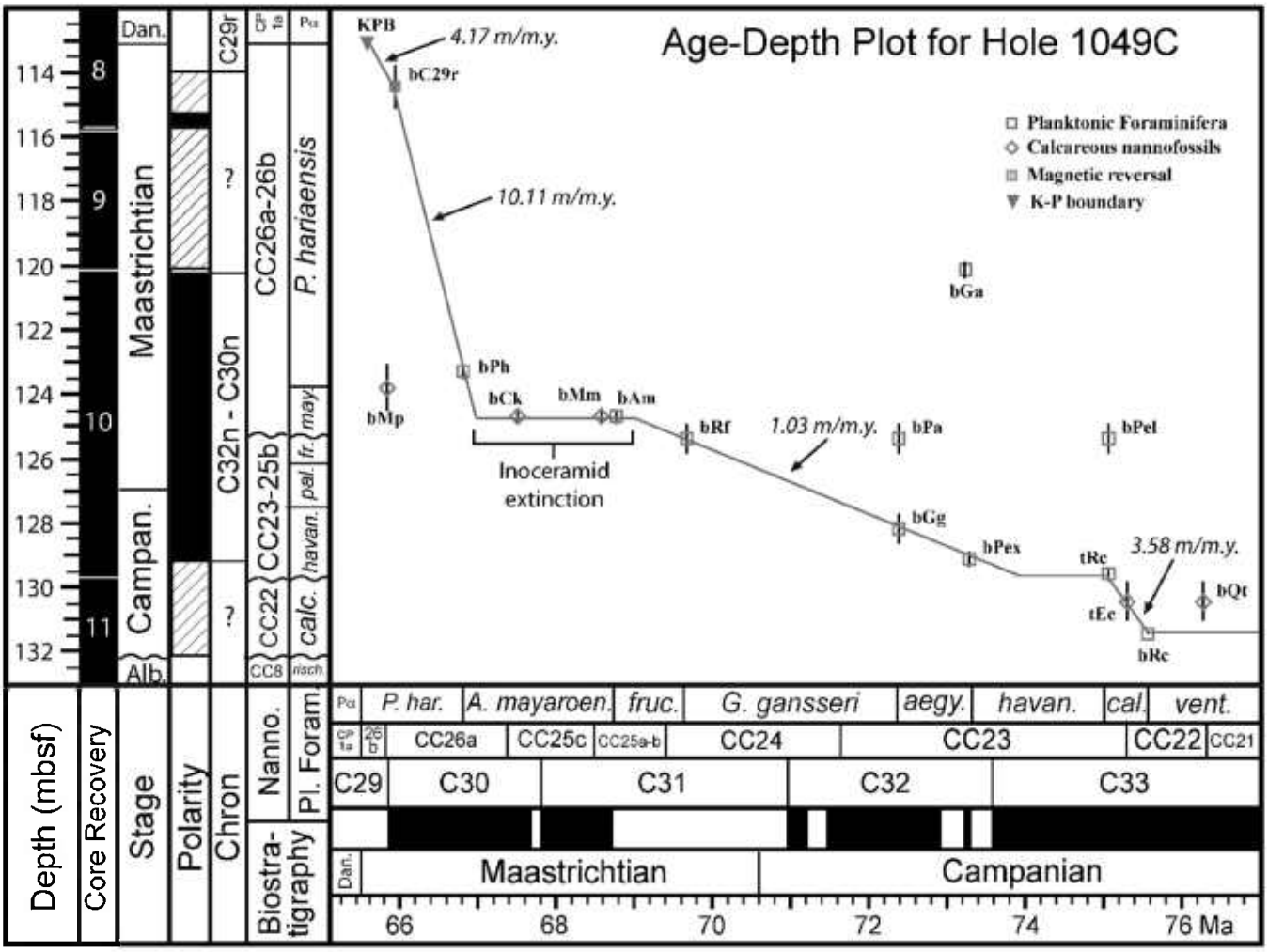

FIGURE 4. Age-depth plot for Hole 1049C. Horizontal axis shows standard tropical/subtropical planktonic foraminiferal and calcareous nannofossil biozones correlated to the Gradstein and others (2004) geologic time scale; vertical axis shows the Blake Nose core-depths, core recovery, magnetostratigraphic interpretations and planktonic foraminiferal and calcareous nannofossil biozones. A line of correlation (LOC) is drawn through the most reliable stratigraphic event data points. Calculated sedimentation rates are shown for each change in slope of the LOC. Stratigraphic uncertainty is plotted as vertical bars for each datum to show the thickness between samples containing the datum marker and the next sample below or above where the datum marker is absent. Wavy lines represent major unconformities. Magnetic polarity intervals are represented by black for normal, white for reversed and diagonal lines for uncertain. Full spelling and explanation of the species datums are presented in Table 1. Inoceramid bivalve extinction level identified in the present study.

Abathomphalus mayaroensis Partial-range Zone (base same, top different from *Abathomphalus mayaroensis* Partial-range Zone of Robaszynski and Caron, 1995)

Definition. Biostratigraphic interval from the LO of *Abathomphalus mayaroensis* to the LO of *Pseudoguembelina hariaensis.*

Magnetochronologic calibration. See above for base. The LO of *P. hariaensis* has been correlated with middle Chron C30n in the Mediterranean region (Robaszynski and Caron, 1995) and lower Chron C30n in the mid-latitude South Atlantic Ocean (Li and Keller, 1998).

Age Estimates. Base 68.72 Ma, top 66.78 Ma.

Remarks. The nominate taxon occurs consistently in low abundance throughout this zone. Characteristic globotruncanid species include *Globotruncana arca*, *Globotruncanita stuartiformis*, *G. stuarti* and *Contusotruncana contusa.* Heterohelicids are dominated by *Heterohelix globulosa*, *H. navarroensis*, *H. planata*, *H. striata* and *Racemiguembelina fructicosa*, whereas *Heterohelix labellosa*, *Pseudoguembelina excolata*, *P. palpebra*, *Planoglobulina multicamerata* and *Pseudotextularia nuttalli* occur consistently in low to moderate abundance. *Rugoglobigerina rugosa* and *R. hexacamerata* are also common in this zone.

The LO of *Trinitella scotti* is recorded in the middle of the *A. mayaroensis* Zone.

Pseudoguembelina hariaensis Partial-range Zone (=*Pseudoguembelina hariaensis* Partial-range Zone of Robaszynski and Caron, 1995)

Definition. Biostratigraphic interval from the LO of the nominate species to the extinction of most Cretaceous

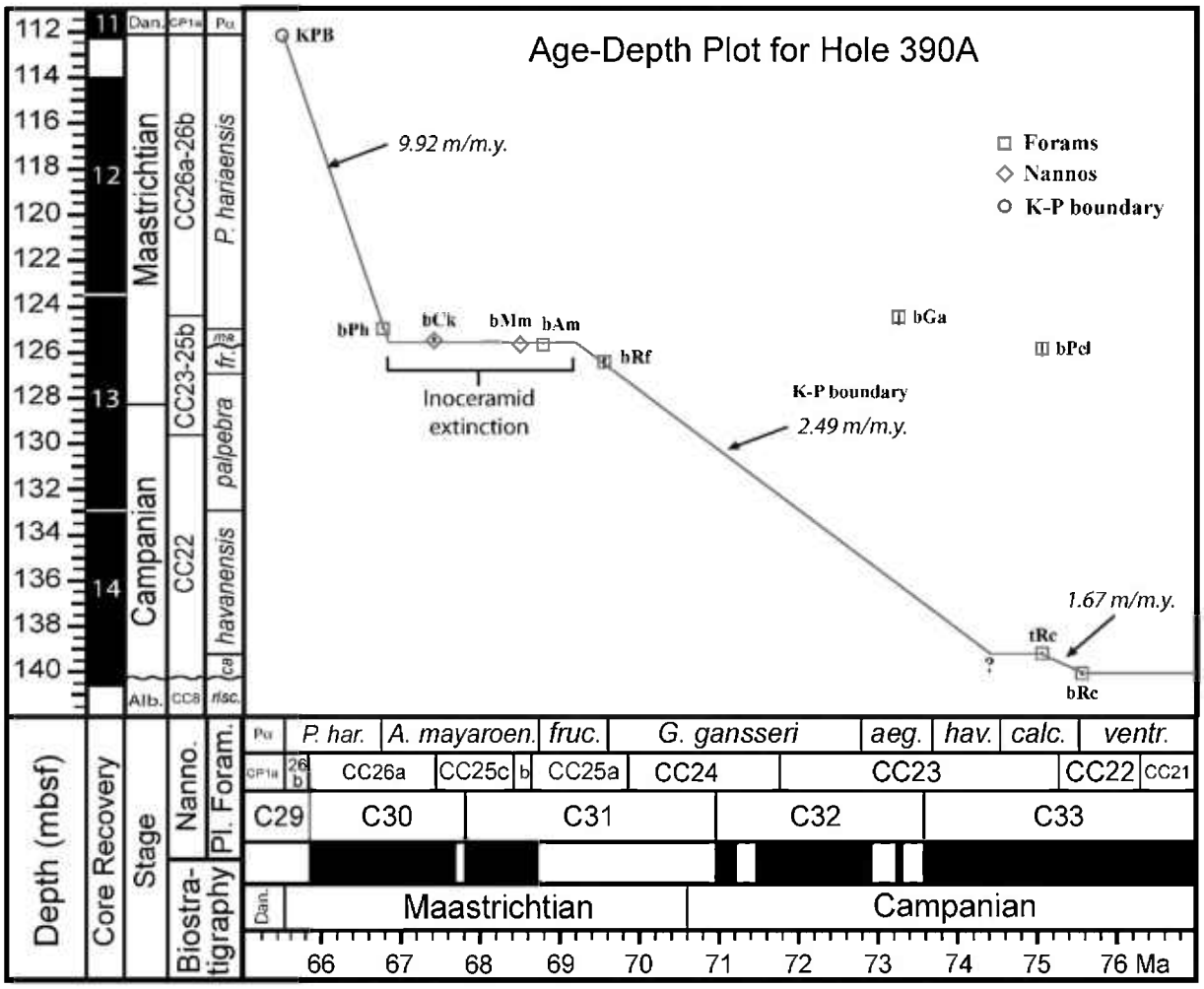

FIGURE 5. Age-depth plot for Hole 390A. Inoceramid bivalve extinction level identified by MacLeod and others (2000). Campanian unconformity identified based on correlation with Site 1049 sections in the absence of datum control points. See caption of Figure 4 for further explanation.

planktonic foraminifera at the Cretaceous-Paleogene boundary.

Magnetochronologic calibration. See above for base. Top correlated with lower Chron C29r (Premoli Silva and Sliter, 1994).

Age Estimates. Base 66.78 Ma, top 65.50 Ma.

Remarks. The nominate taxon occurs consistently throughout the interval in relatively moderate abundance. Globotruncanid species include common *Globotruncanita stuartiformis*, *Globotruncana arca* and *Contusotruncana contusa*; rare to moderately abundant *Globotruncanita stuarti*, *Globotruncana falsostuarti*, *G. esnehensis*, *G. conica* and *G. angulata*; and very rare *Abathomphalus mayaroensis*, *Globotruncana dupleublei* and *G. insignis*. Heterohelicids are dominated by *Heterohelix globulosa* and include relatively common *Heterohelix labellosa*, *Racemiguembelina fructicosa*, *Pseudotextularia elegans* and *P. nuttalli*.

The HOs of *Globotruncana linneiana* and *Contusotruncana patelliformis* occur in the base and middle of this zone, respectively.

Plummerita hantkeninoides is absent from all of the Blake Nose sites despite the presence of sediments spanning the age range of this species, which evolved within the last 300 k.y. of the Maastrichtian (Abramovich and Keller, 2002). This species apparently preferred to live in eutrophic shelfal to upper-slope continental margin environments (e.g., Abramovich and others, 1998; Abramovich and Keller, 2002; MacLeod and others, 2007) and has not been reported from open–ocean pelagic carbonate sediments.

AGE MODELS

Datums determined for Campanian-Maastrichtian planktonic foraminifera and calcareous nannofossils and the levels of magnetic polarity reversals obtained from DSDP/ODP sites on the Blake Nose provide the basis for construction of the age-depth models presented in Figures 4–7. Age assignments, lowest and highest occurrence

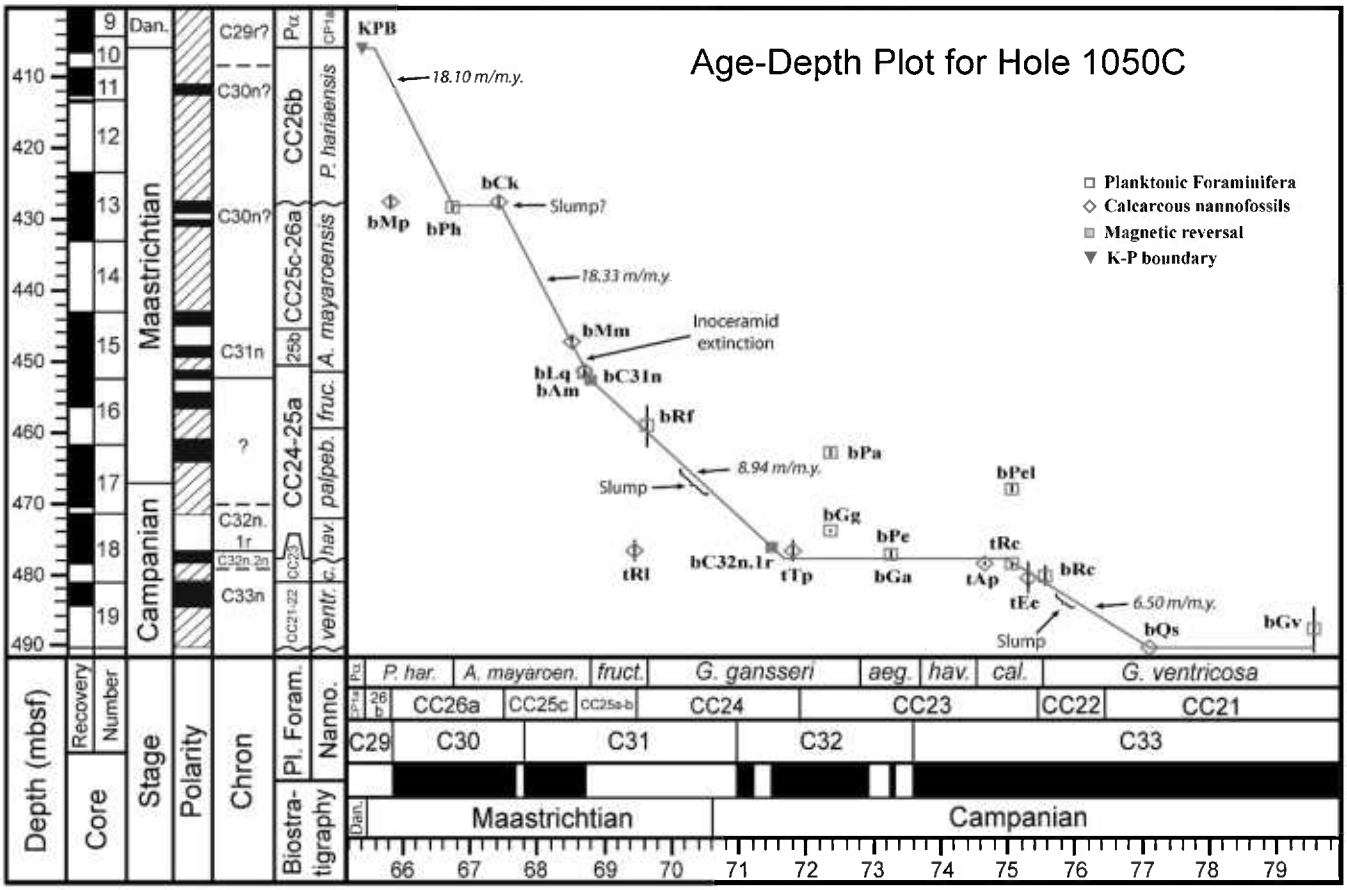

FIGURE 6. Age-depth plot for Hole 1050C. Inoceramid extinction level identified by MacLeod and Huber (2001b). See caption of Figure 4 for further explanation.

depths, and reference sources are presented in Tables 2–5. Sr isotopic data are used as a means of independently evaluating the model and are discussed below.

SITE 1049

Cretaceous sediments from the three holes drilled at Site 1049, which are located about 10 m apart from each other, are precisely correlated using the base of the impact bed at the Cretaceous/Paleogene (K/P) boundary as a datum plane (Fig. 2). Constructing a precise age model for this site (and for Hole 390A) is difficult as the section is relatively thin (reducing stratigraphic resolution) and contains significant coring gaps and disturbed bedding that may indicate slumping in places. Sediment thickness between the K/P boundary and the unconformity bounding the late Campanian *Radotruncana calcarata* Zone and the early Albian *Hedbergella rischi* Zone varies between 17.98 and 19.26 m in the three drillholes, but it is about 10-m thicker in Hole 390A due to a thicker interval of Campanian sediment (Fig. 2). Sub-bottom depths to the K/P boundary differ between these holes by as much as 14.8 m. This offset probably resulted from error in calculating the depth to the seafloor surface, as the method used at Site 1049 depended on estimation of when a reduction in drill string weight occurred (Norris and others, 1998, p. 49), which can be imprecise when drilling in soft sediment. Comparison of sub-bottom depths for planktonic foraminiferal and calcareous nannofossil datums for these holes show offsets that are similar to the boundary offsets. Planktonic foraminiferal and calcareous nannofossil datums were determined with greatest precision at Hole 1049C, which is used as the basis for constructing the age model for Site 1049 (Fig. 4). Table 2 lists all datums included in this age model along with the less precisely determined datums used to determine zonal boundary depths for Holes 1049A and 1049B (Fig. 2).

Despite the problems outlined, the age model for Hole 1049C is constrained by a number of reliable datums. The depths of the K/P boundary and the Chron C29r/C30n reversal in the uppermost Maastrichtian establish a sedimentation rate of 4.17 m/m.y. Below the base of Chron C29r, the estimated sedimentation rate increases to 10.11 m/m.y., as determined by passing the LOC through the FAD of *Pseudoguembelina hariaensis*. This datum occurs at the same level as the FAD of the calcareous nannofossil *Micula prinsii* and just above a distinct sediment color change at 125.48 mbsf that is interpreted as a hiatal surface. Based on co-occurring FADs of four planktonic foraminiferal and calcareous nannofossil datums, this hiatus is estimated to span the interval from 66.92 to 68.95 Ma.

Between 68.95 Ma and 73.90 Ma, planktonic foraminiferal datums line up to define a LOC that suggests

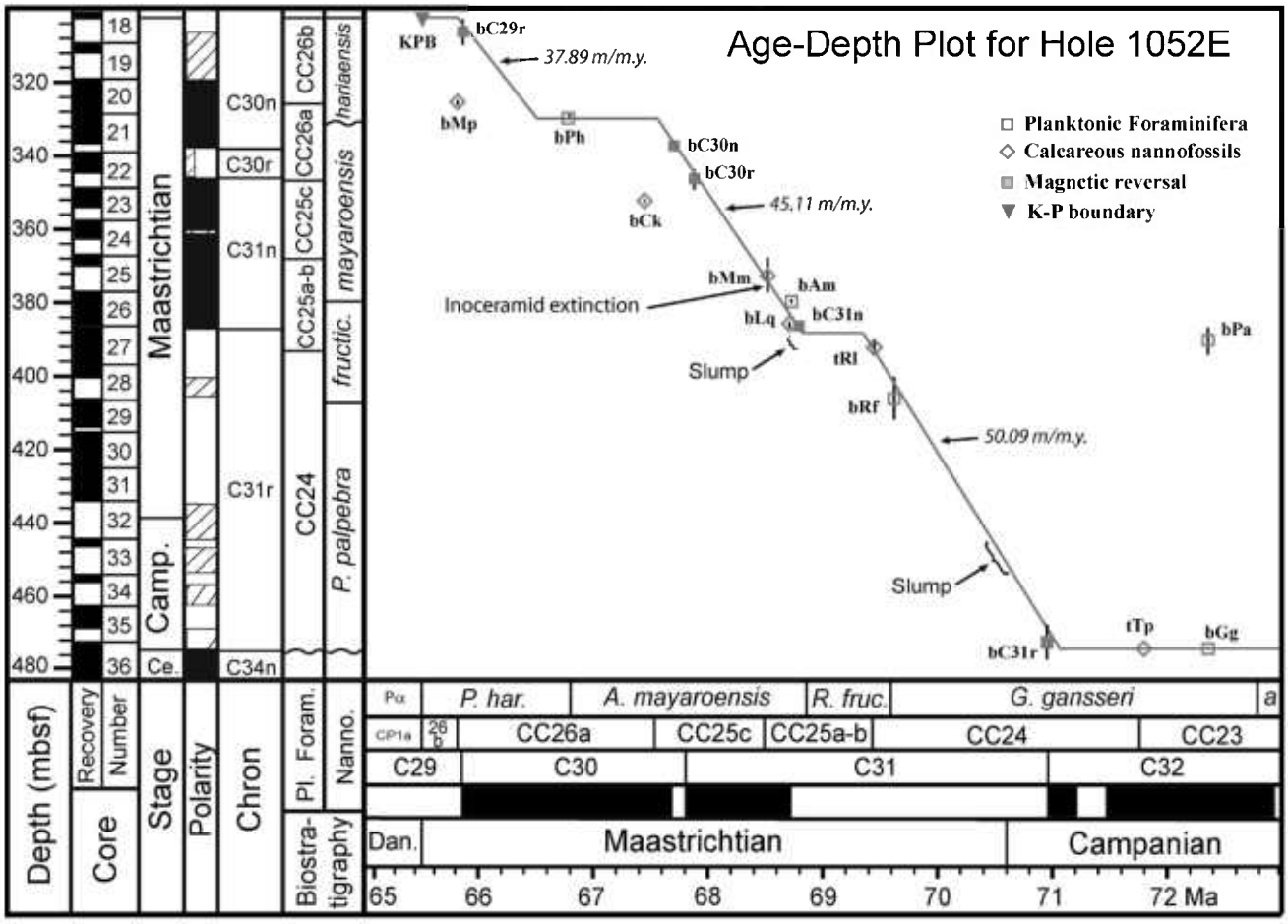

FIGURE 7. Age-depth plot for Hole 1052E. Inoceramid bivalve extinction level identified by MacLeod and Huber (2001b). See caption of Figure 4 for further explanation.

sedimentation rates were much slower (1.03 m/m.y.) below the color change than above it (10.11 m/m.y.). Disturbed bedding in this interval is suggestive of slumping, but there is no biostratigraphic evidence for mixing or repetition of strata. A short (~1.14 m.y.) hiatus is placed between the base of the *G. havanensis* Zone and top of the *R. calcarata* Zone, below which is a 2-m interval that spans most of the *R. calcarata* Zone. An ~34-m.y. unconformity separates upper Campanian from lower Albian sediments.

The LOs of *Planoglobulina acervulinoides* and *Pseudotextularia elegans* are estimated as 69.62 Ma according to the LOC for Hole 1049C. This age is much younger than the FAD ages that have been previously used for these species (Table 1).

SITE 390A

The age-depth curve for Hole 390A is very similar to that of Hole 1049C. Differences between the two curves are attributed to inclusion of fewer calcareous nannofossil datums and absence of the Chron C29r/C30n paleomagnetic control point in Hole 390A (Fig. 5). The K/P boundary, which is used as a datum plane for correlation of the three holes at Site 1049, was not recovered intact at Site 390 because of coring disturbance (Benson and others, 1978). The boundary is placed between 145 and 149 cm in Section 390A-11-5 (111.95–112.00 mbsf), where there is a sediment color change and a mixture of planktonic foraminifera and calcareous nannofossils of latest Maastrichtian and earliest Danian age (Benson and others, 1978).

The age model for Hole 390A indicates an initially fast sedimentation rate of 10.11 m/m.y. between the K/P boundary (KPB) and the mid-Maastrichtian unconformity, which is marked by a sharp color change at 125.87 mbsf. The unconformity is estimated to span the interval between 66.94 and 68.85 Ma, with a 1.91-m.y. duration. Below the unconformity, the sedimentation rate slows to about 1.03 m/m.y. A brief unconformity between 75.05 and 73.90 Ma is followed by a short interval of sedimentation and then a major unconformity between 75.57 Ma and 110.00 Ma.

There are significant differences in depths below the seafloor between Holes 390A and 1049C that should be considered when correlating between these two holes (Fig. 2). First, assuming the KPB is nearly complete at Hole 390A, its depth is 1.08 m above the base of the tektite bed at Hole 1049C. Second, the depth of the mid-Maastrichtian unconformity Hole 390A is 1.47 m below that in Hole 1049C. Finally, biozones below the mid-Maastrichtian unconformity at Site 390A thicken with depth, such that the top of the *R. calcarata* Zone is 8.95 m deeper than in Hole 1049C. These differences suggest that

the position of Hole 390A must be offset relative to Site 1049, despite use of the same geographic coordinates. These differences underscore the problems of resolving short intervals of time in sections with slow sedimentation rates and potential sedimentological complications.

Site 1050

The most complete Campanian-Maastrichtian record at the Blake Nose occurs at Site 1050, extending ~79 m from the *G. ventricosa* Zone to the *P. hariaensis* Zone. Although the K/P boundary is biostratigraphically complete, no impact ejecta were observed in sediments above or below the boundary layer, suggesting that the impact bed may have been slumped away (Norris and others, 1998). As observed at Site 1049, the LOs of *M. prinsii* and *P. hariaensis* occur in close proximity to each other, and the latter is used as a control point for the LOC. The sedimentation rate for this interval is estimated as 18.10 m/m.y. A 0.66-m.y. hiatus is interpreted to occur at a possibly slumped interval at 427.75 mbsf. Tie points linking the LO of *C. kamptneri* and the Chron C31n/C31r boundary are supported by several calcareous nannofossil and planktonic foraminiferal datums, and indicate a sedimentation rate of 18.33 m/m.y. within the *A. mayaroensis* Zone.

From the base of Chron C31n to the base of the *G. havanensis* Zone, the planktonic foraminiferal and calcareous nannofossil datums indicate a sedimentation rate of 8.94 m/m.y. The LOs of *Planoglobulina acervulinoides* and *Pseudotextularia elegans* are about 69.98 and 68.76 Ma, respectively, according to the LOC at Hole 1050C. These ages are considerably younger than the FAD ages that have been used previously for these species (Table 1).

Similarly, the LO of *Reinhardtites levis* at Site 1050 is recorded at a level that projects to about 2.02 m.y. earlier than its previously assigned FAD age.

A hiatus estimated to range from 75.04 to 71.62 Ma spans the lower *G. havanensis* Zone and upper *R. calcarata* Zone. Below this hiatus is a 13.42-m interval comprising the interval from the *R. calcarata* Zone to the *G. ventricosa* Zone and for which the estimated sedimentation rate is 6.50 m/m.y. This interval is underlain by a disconformity ~10 m.y. in duration that separates upper Campanian from lower Cenomanian sediments.

Site 1052

The 172-m-thick, late Campanian-Maastrichtian interval at Hole 1052E ranges from the *G. havanensis* Zone to the *P. hariaensis* Zone. The K/P boundary was not recovered in this hole, probably because of poor core recovery, but the upper Maastrichtian is considered biostratigraphically complete (Norris and others, 1998). The LOC spanning the *P. hariaensis* Zone is determined from alignment of the FAD of *P. hariaensis* and the base of Chron C29r. As observed at Sites 1049 and 1050, the LO of *M. prinsii* is very close to that of *P. hariaensis*, contrary to the 0.54-m.y. age difference that has been assigned to these species. Based on this curve, we estimate that sediment from the last 150 k.y. of the Maastrichtian is missing. The sedimentation rate in this interval is calculated as 37.89 m/m.y. As occurs at Sites 1049 and 1050, a hiatus is recognized just below the LO of *P. hariaensis* and ranges from 66.49 to 67.57 Ma. Alignment of the bases of Chrons C30n and C30r and calcareous nannofossil and planktonic foraminiferal datums establishes a sedimentation rate of 45.11 m/m.y. and indicates the presence of a hiatus spanning the period from 69.34 to 68.82 Ma, which is within a slumped interval in Core 1052E-17.

Using the FAD of *R. fructicosa* and the base of Chron C31r as tie points, the sedimentation rate between the lower *R. fructicosa* Zone and the upper *G. havanensis* Zone is calculated as 50.09 m/m.y. A major unconformity that separates the upper *G. havanensis* Zone from the *Rotalipora globotruncanoides* Zone (lower Cenomanian) in Section 1052E-36R-1 is estimated to have a duration of ~26 m.y.

A delayed first occurrence at Site 1052 for *C. kamptneri* (or unrecorded occurrence) is suggested by an LO that is 0.59 m.y. younger than the assumed age of its FAD. The LOs of *P. acervulinoides* and *P. elegans* are dated as 69.05 and 68.68 Ma, respectively, according to the LOC for Hole 1052E. These ages are much younger than the FAD ages that have previously been used for this species.

DISCUSSION

Biostratigraphic Datums

The age models constructed for the upper Campanian-Maastrichtian interval at each of the Blake Nose drill sites demonstrate that the relative order of occurrences and ages used for most of the planktonic foraminiferal and calcareous nannofossil datums listed in Table 1 are consistent and reliable. Moreover, the Maastrichtian magnetic-reversal-boundary tie points that are included in the age models are collinear with the microfossil datums, providing further evidence that the biostratigraphic age calibrations are dependable, at least for tropical and subtropical oceans.

Three out of the thirteen calcareous nannofossil species used in construction of the age models show significant offsets from the age model LOCs from at least one of the three drill sites where they have been identified. The HO of *Reinhardtites levis* in Hole 1050C was identified 18.32 m lower than the depth predicted from the LOC (Fig. 6) and the LO of *Ceratolithoides kamptneri* was identified 19.41 m lower than the depth predicted by the LOC in Hole 1052E (Fig. 7). These inconsistencies do not necessarily point to a problem with the assigned datum ages, since there is good agreement with the age models at the other Blake Nose sites. However, at all three Leg 171B drill sites, the assigned FAD age for *Micula prinsii* is consistently younger by about 0.5 m.y. than the predicted age for its LO. This discrepancy is difficult to explain since the *M. prinsii* datum was carefully documented by Henriksson (1993) in multiple Atlantic and Pacific Ocean sequences with magnetostratigraphic age control.

Significant offsets from the age model lines of correlation are shown for several planktonic foraminiferal datums at all of the Blake Nose sites. Relative to the LOCs for each site, the LO of *Pseudotextularia elegans* projects to ages that are

5.5 to 6.4 m.y. younger than the assigned datum age, and the LO of *Planoglobulina acervulinoides* is between 2.4 and 3.3 m.y. too young. Both of these offsets are probably an artifact of inconsistency in taxonomic concepts. The confusion with *P. elegans* stems from a poorly drawn type specimen that has been lost. For this species, we follow the species concept of Nash (1981), who selected a neotype bearing thick, continuous costae. As was noted by Nederbragt (1991), *P. elegans* has a distinctively different appearance from the finely costate *Pseudotextularia nuttalli*, and the stratigraphic ranges differ in that the former species is restricted to the Maastrichtian and the latter species ranges down to the Coniacian. The 75.25-Ma age for the FAD of *P. elegans* that was cited in Chart 5 of Hardenbol and others (1998) was most likely based on identification of the finely costate *P. nuttalli*. Based on the Blake Nose age models, the LO of *P. elegans* ranges between 68.68 and 69.62 Ma, and has a mean age of 69.02 Ma (Table 7). Similarly, it is likely that the older age reported for the FAD of *P. acervulinoides* in Gradstein and others (2004) is based on a species concept that includes forms here assigned to *Planoglobulina riograndensis*. We differentiate *P. riograndensis* as having vermicular ornamentation and a greater number of multiserial chambers than does *P. acervulinoides*. Based on our observations, the LO of *P. acervulinoides* occurs between 69.05 and 69.98 Ma, with an average age of 69.55 Ma calculated from all the Blake Nose drill sites. At the Blake Nose, we have determined that the LO of *P. riograndensis* is in the upper *R. calcarata* Zone, with an FAD of 75.72 Ma. This age is consistent with the range reported for *P. riograndensis* by Nederbragt (1991).

Variations in the LOs of *Globotruncana aegyptiaca* and *Gansserina gansseri* among sections and relative to the established ages of the FADs are explained as sampling artifacts due to the scarcity of these taxa at the Blake Nose. The LO of *G. aegyptiaca* in Hole 1049C is recorded in the middle of the *P. hariaensis* Zone, plotting about 7.1 m.y. younger than the assigned FAD age; in Hole 1050C, the LO of *G. aegyptiaca* is in the *G. havanensis* Zone and plots 1.58 m.y. younger than the assigned age; and in Hole 1052, the LO is in the upper *P. palpebra* Zone and plots 3.35 m.y. younger than the assigned age. The LO of *G. gansseri* is recorded close to its FAD age in Hole 1049C, but its occurrence in Hole 1050C is over 1 m.y. younger than its assigned datum age. In Hole 1052E, the lower range of *G. gansseri* is truncated by a disconformity.

In addition to the taxa used to constrain the LOC at various sections, a number of additional planktonic foraminifera are considered reliable regional chronostratigraphic biomarkers. These taxa are listed in Table 7 along with their depths and ages calculated from each of the age models. Mean ages and maximum difference between ages are also presented. Although *Contusotruncana contusa* has been used as a zonal marker taxon in some studies (e.g., Wonders, 1980; Li and Keller, 1998, 1999), the 1.06-m.y. difference in ages for its LO at the Blake Nose reflects the difficulty in consistently identifying this species because of its morphologic variability (e.g., see Kucera and Malmgren, 1996).

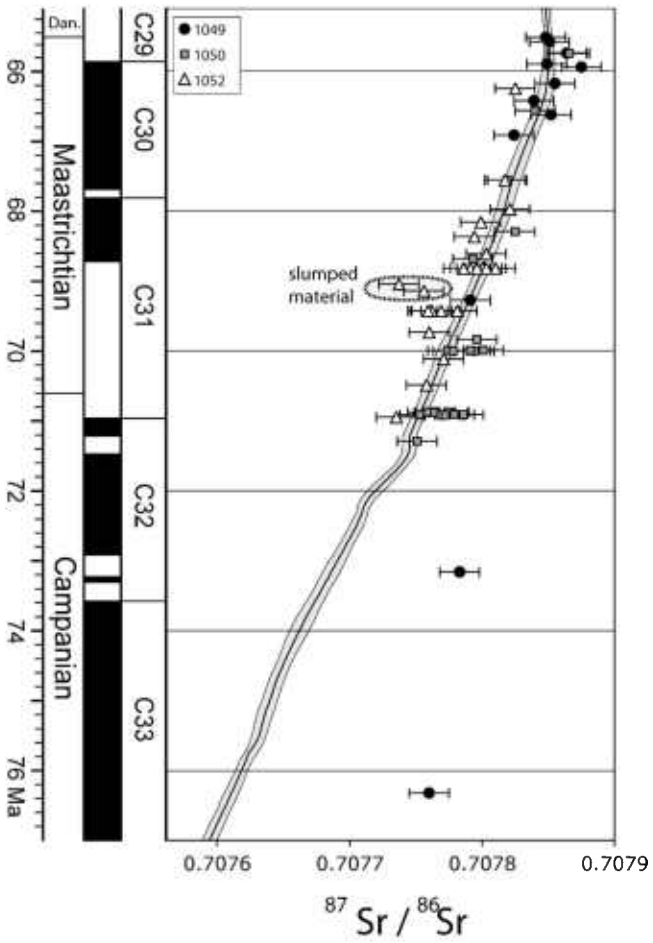

FIGURE 8. Campanian and Maastrichtian strontium isotopic data from MacLeod and others (2003) plotted against age of the samples estimated using the age models. Seawater curve of McArthur and Howarth (2004) shifted by 0.000020 (see text) is shown by the heavy curved line with estimated error on the curve represented by the gray shading. Error bars on individual data points represent ± 2 s.d. of analytical precision.

COMPARISON BETWEEN AGE MODELS AND SR-ISOTOPIC DATA

Agreement between the age models and Sr isotopic data is generally excellent (Fig. 8). Because the seawater curve was calibrated to the timescale of Gradstein and others (2004) separately from data used to construct the age models and because Sr-isotopic measurements do not depend in any way on chronostratigraphic assignments, this comparison is an independent confirmation of the general accuracy of the age models. Beyond this confirmation, the Sr plot indicates intervals where uncertainty in age estimates are relatively large (where the age models and Sr ages are not congruent) and intervals where age uncertainty is likely low (where the age models and Sr ages are congruent).

In this regard, recognition that much of the lower *Abathomphalus mayaroensis* Zone is missing in Hole 1049C results in better agreement between Sr data and biostratigraphy than seen in a similar comparison using a simple age model (MacLeod and others, 2003) and suggests improved precision of age estimates in the upper Maas-

trichtian in Hole 1049C. The largest discrepancy between the two estimates occurs in the lower portion of the section in Hole 1049C where Sr-based age estimates that would place the samples in the lower Maastrichtian are at odds with the presence of the lower Upper Campanian marker *R. calcarata*. Possible explanations for this discrepancy include reworking of older zonal markers into younger sediment and alteration of original $^{87}Sr/^{86}Sr$ ratios. The former is consistent with disturbed bedding observed in portions of Cores 1049C-10 and -11 but is difficult to reconcile with the ordered sequence of both highest and lowest occurrences that define the LOC. The latter is consistent with the coarser nature of the sediment below the color change within Core 10 in Hole 1049C, which might allow relatively easy circulation of pore fluids carrying a higher $^{87}Sr/^{86}Sr$ ratio.

Other discrepancies are minor by comparison. Within the major slumped interval in Hole 1052E (~69 Ma), two Sr analyses suggest the slumped material includes material older than the subjacent hemipelagic interval (MacLeod and others, 2003) and the five analyses immediately below the slump suggest the youngest sediment below the slump may be ~0.5 m.y. older than estimated biostratigraphically. Similarly, the high-resolution samples bracketing the major slump in Hole 1050C suggest bracketing ages up to ~0.5 to 1.0 m.y. younger than those estimated in the age models. In both cases, the presence of slumped intervals and significant coring gaps below the LO of *Racemiguebelina fructicosa* affect the precision of the LOC used in the age models for these intervals. Finally, the highest point in Hole 1052E suggests that the hiatus spanning the K/P boundary in this hole could be slightly longer than estimated, but coring gaps in cores 1052E-18 and -19 again limit the precision possible in this interval.

Sedimentation History

The age-depth curves generated from the Blake Nose sites suggest a varied depositional history in the upper Campanian and Maastrichtian across the Blake Nose depth transect and through time. At the deepest and most-offshore site (Sites 1049 and 390), the upper Maastrichtian sedimentation rate is relatively high (~10.11 m/m.y.) for a sequence with almost no terrigenous clastic content. This interval could indicate a period of increased calcareous plankton productivity, or it could reflect deposition during a period characterized by both downslope and pelagic input, and it could be related to hiatuses observed within the late Maastrichtian at Sites 1050 and 1052. However, core photographs from Cores 1049C-8 through -10 do not show slump features nor is there microfaunal evidence for downslope transport. The dramatic slowing in sedimentation rate from 10.11m/m.y. to 1.03 m/m.y. across the 66.94–68.85 Ma unconformity at Site 1049 (Fig. 4) suggests that the cause(s) of high sedimentation rates ceased prior to the K/P boundary. Study of benthic foraminiferal assemblages could help determine whether significant bottom-water changes occurred across this unconformity, which is evident at all three Blake Nose drill sites.

Although there are several slumped intervals in the upper Campanian-Maastrichtian cores at Sites 1050 and 1052, the age estimates presented are equivocal as to whether these occurred as discrete local events or are correlative and potentially related to regional paleoceanographic changes. Several slumps in Hole 1052 have no apparent counterparts in the other sites and, as discussed above, it is difficult to evaluate the nature of disturbed bedding (e.g., drilling disturbance or slumping) in the lower Maastrichtian at Hole 390A and Site 1049. On the other hand, the mid-Maastrichtian hiatus at Site 390A/1049 and the missing section in the major slump in Hole 1052E have very similar age estimates at their bases. Further, if Sr ages for the major slump in Hole 1050C are more accurate than the age models, this interval would correlate closely with the slump in Hole 1052E. Regardless, the continuity of all age estimates—above and below the slumps and hiatuses—supports the conclusion of MacLeod and others (2003) that the pre-KPB slumped intervals on the Blake Nose were not generated by seismic shaking during the K/P impact event as had been proposed based on geophysical data (Klaus and others, 2000; Norris and others, 2000; Norris and Firth, 2001).

At all four sites on the Blake Nose, the oldest Campanian sediments are bounded below by major unconformities. The age models constructed for these sites in this study and by previous workers (Bellier and others, 2000; Petrizzo and Huber, 2006) indicate that this unconformity spans the period from about 76–110 Ma at Site 1049, 77–87 Ma at Site 1050, and 72–97 Ma at Site 1052. Closing of east-west gateways to Tethyan circulation and opening of an increasingly unrestricted north-south passage through the tropical Atlantic gateway are possible ultimate causes for these unconformities. Because this study only examined material above the unconformity, though, we lack observations that meaningfully address the issue.

Paleoceanographic and Biotic Events

Stable isotope data generated from the upper Campanian-Maastrichtian interval along the Blake Nose depth transect are replotted in Figures 9 and 10 using ages calculated from the new age models discussed above. For Hole 390A, these new age assignments reveal that the age span of stable isotope and benthic foraminiferal abundance data generated by Friedrich and others (2004) and Friedrich and Hemleben (2007), respectively, was underestimated by over 3.5 m.y. These authors assigned samples between horizons 390A-14-5, 70 cm and -13-2, 53 cm (139.71–125.93 mbsf) to the lower Maastrichtian and assigned an age range from 71.3 to 69.6 Ma using the Gradstein and others (1994) time scale. Their age assignments were based on the assumptions that this stratigraphic interval correlates with the *Globotruncana falsostuarti-Gansserina gansseri* Zone and that sedimentation was continuous and averaged 1.2 m/m.y. However, the revised age model for Hole 390A suggests (1) the oldest sample in their study correlates with the *Radotruncana calcarata* Zone and should be assigned an age of 74.56 Ma, (2) the youngest sample correlates with the *Racemiguembelina fructicosa* Zone and should be assigned an age of 69.33 Ma, (3) a 0.42-m.y. unconformity occurs at 139.36 Ma and marks the top of the *R. calcarata* Zone, and (4) the sedimentation rate above the

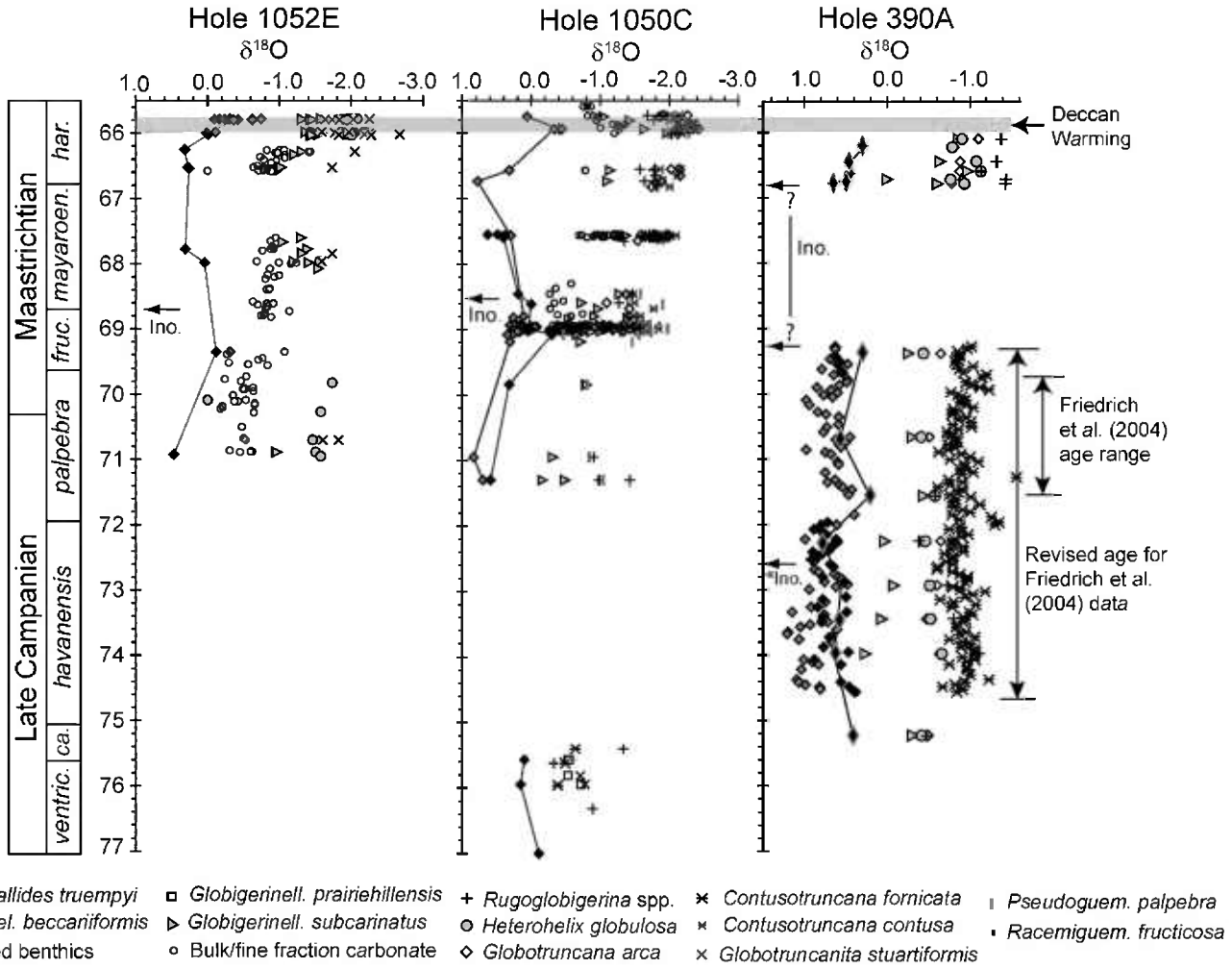

FIGURE 9. Revised ages for previously published oxygen isotope data spanning the late Campanian-Maastrichtian from deep-sea sites drilled along the Blake Nose depth transect. Planktonic foraminiferal biozone abbreviations include *ventric.* = *Globotruncana ventricosa* Zone; *ca.* = *Radotruncana calcarata* Zone; *palpebra* = *Pseudoguembelina palpebra* Zone; *mayaroensis* = *Abathomphalus mayaroensis* Zone; *har.* = *Pseudoguembelina hariaensis* Zone. Stable isotope data for Holes 1052E and 1050C from MacLeod and Huber (2001), MacLeod and others (2001) and Isaza-Londoño and others (2006). Hole 390A stable isotope data from MacLeod and others (2000; mixed benthics: *Globotruncana arca*, *Heterohelix globulosa*, *Globigerinelloides subcarinatus* and *Rugoglobigerina* spp.) and Friedrich and others (2004: all other data). Upper inoceramid extinction level ("Ino.") identified by MacLeod and others (2000), lower extinction level (= *Ino.) by Friedrich and others (2007). See text for additional discussion.

R. calcarata Zone averaged 2.49 m/m.y. Therefore, Friedrich and Hemleben (2007) underestimate by over 3 million years the amount of time for major reorganization of deep- and intermediate-water circulation. Similarly, Friedrich and Hemleben (2007) identified a major decline in inoceramid abundance at 134.5 mbsf, which is 8.63 m below the inoceramid extinction level observed by MacLeod and others (2000) in Hole 390A. According to the new age model, this inoceramid decline should be assigned an age of 72.6 Ma, which is 3 m.y. earlier than the age assigned by Friedrich and Hemleben (2007). Absence of upper Campanian sediments older than 71.62 Ma at Sites 1050 and 1052 (Table 6) prevents an opportunity to test whether this inoceramid abundance change occurred at shallower depths on the Blake Nose.

The inoceramid bivalve extinction event observed within the lowermost *Abathomphalus mayaroensis* Zone in Holes 1052E and 1050C (MacLeod and Huber, 2001) is now age dated between 68.5 and 68.7 Ma. This is in good agreement with the 68.6–68.9 Ma age for this extinction event reported by Frank and others (2005) at three sites on the Shatsky Rise. Published $\delta^{18}O$ and $\delta^{13}C$ data obtained from benthic and planktonic foraminifera and from bulk and fine-fraction carbonate do not show significant positive or negative shifts that correlate with the inoceramid extinction (Figs. 9, 10). Thus, the hypothesis that major shifts in source regions and circulation patterns for intermediate and deep water promoted the decline or extinction of the inoceramid bivalves (e.g., MacLeod, 1994; MacLeod and Huber, 1996; Frank and Arthur, 1999; MacLeod and others, 2000; Friedrich and others, 2004; Friedrich and Hemleben, 2007; Frank and others, 2005) is not supported by the combined results obtained from the Blake Nose. However, if the mid-Maastrichtian hiatus at Hole 390A and Site 1049 is coincident with and causally related to the slumps at 1050C and 1052E, it is possible that at the Blake

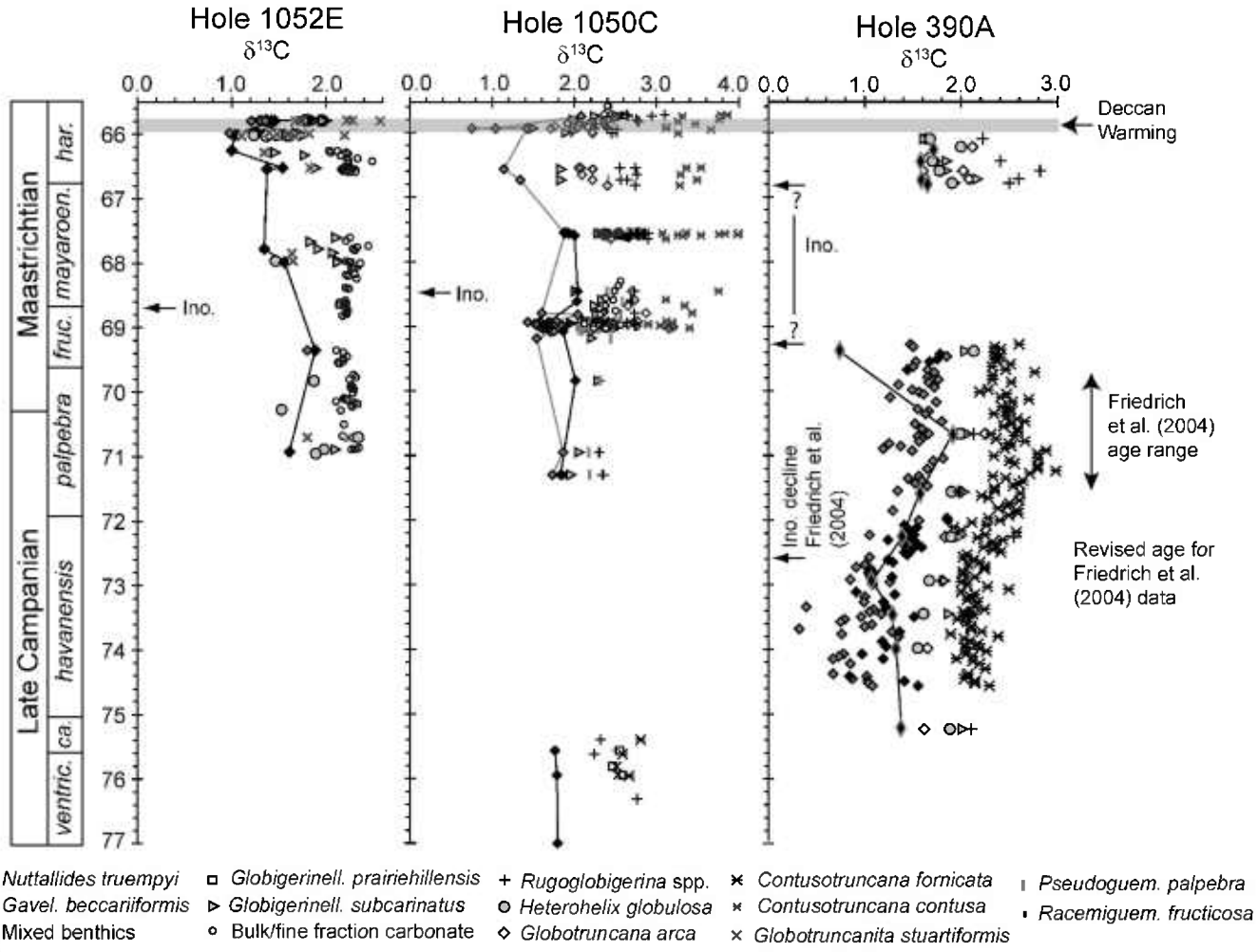

FIGURE 10. Revised ages for previously published carbon isotope data spanning the late Campanian-Maastrichtian from deep-sea sites drilled along the Blake Nose depth transect. See caption for Figure 8 and text for explanation.

TABLE 6. Age and duration (m.y.) of upper Campanian-Maastrichtian unconformities on the Blake Nose.

Base (Ma)	Top (Ma)	Duration (m.y.)
	Hole 390A	
69.22	66.86	2.35
75.04	74.62	0.42
110.00	75.55	34.45
	Hole 1049C	
68.85	66.94	1.91
75.05	73.90	1.15
110.00	75.57	34.43
	Hole 1050C	
65.56	65.50	0.06
67.44	66.78	0.66
75.04	71.62	3.42
87.30	77.10	10.20
	Hole 1052E	
65.78	65.50	0.23
67.52	66.49	1.03
69.34	68.82	0.52
96.80	71.04	25.76

Nose the manifestation of changing circulation patterns is sedimentological and not evidenced by isotopic changes.

The updated stable isotope plots for Holes 1052E and 1050 support the claim (Wilf and others, 2003) that a 0.6 to 0.8‰ negative shift in benthic and planktonic foraminiferal $\delta^{18}O$ values (~3°C warming) between 65.90 and 65.65 Ma. (Fig. 9) was synchronous with the onset of Deccan volcanism, which began at the base of Chron C29R (Courtillot and others, 1986; Hansen and others, 1996). This oxygen isotopic warming event has not been observed at Site 390 because published stable isotope data terminate below this time interval.

CONCLUSIONS

Age-depth models are created for the upper Campanian-Maastrichtian interval recovered from DSDP/ODP Holes 390A/1049C and ODP Holes 1050C and 1052E, which were drilled along a middle to upper bathyal depth transect on the Blake Nose in the subtropical North Atlantic Ocean. These age models are constructed using published and reinterpreted magneto-, chemo-, and biostratigraphic datums along with new biostratigraphic observations, all of

TABLE 7. Depths and calculated ages for secondary planktonic foraminiferal datums identified in the Blake Nose drillholes. Age difference between maximum and minimum ages shown in parentheses. Dashes shown where datum age is uncertain because of the presence of an unconformity.

		Hole 1049C			Hole 1050C			Hole 1052E			
Planktonic foraminifer species	Datum	Top depth (mbsf)	Bottom depth (mbsf)	Age (Ma)	Top depth (mbsf)	Bottom depth (mbsf)	Age (Ma)	Top depth (mbsf)	Bottom depth (mbsf)	Age (Ma)	Mean age (Ma)
Gansserina gansseri	LAD	113.20	113.47	65.57	412.50	412.96	65.95	320.04	322.02	66.27	65.93 (0.70)
Contusotruncana patelliformis	LAD	125.47	125.56	–	413.70	413.88	66.00	324.91	326.02	66.40	66.20 (0.40)
Globotruncana linneiana	LAD	125.47	125.56	–	428.93	429.99	67.53	367.94	368.85	68.19	67.86 (0.66)
Globotruncana bulloides	LAD	125.56	126.54	–	452.50	454.08	68.83	358.54	354.72	67.94	68.34 (0.89)
Contusotruncana fornicata	LAD	125.56	126.54	–	452.18	452.50	68.78	383.49	384.73	68.54	68.66 (0.24)
Pseudotextularia elegans	FAD	125.56	126.54	66.62	451.82	452.18	68.76	388.24	391.27	68.68	69.02 (0.94)
Planoglobulina acervulinoides	FAD	125.56	126.54	69.62	462.17	463.55	69.98	393.09	394.26	69.05	69.55 (0.93)
Planoglobulina multicamerata	FAD	125.56	126.54	69.62	465.74	467.20	70.41	423.27	424.22	70.06	70.03 (0.79)
Contusotruncana contusa	FAD	127.03	128.00	71.04	462.17	463.55	69.98	434.61	445.22	70.39	70.47 (1.06)
Racemiguembel. powelli	FAD	127.03	128.00	71.04	481.69	482.24	–	455.97	465.12	70.92	70.98 (0.12)
Pseudoguembel. kempensis	FAD	126.54	127.03	70.33	465.12	468.27	73.26	465.12	468.27	70.91	71.50 (2.93)
Pseudoguembel. palpebra	FAD	128.00	128.49	71.75	476.55	478.15	71.54	473.70	474.30	–	71.64 (0.21)
Pseudoguembel. excolata	FAD	130.20	130.70	73.89	476.55	478.15	74.90	–	–	–	74.40 (1.01)

which are age calibrated using the Gradstein and others (2004) geomagnetic time scale. The revised age models enable greater accuracy in chronostratigraphic correlation, characterization of changes in sedimentation rates, and determination of the stratigraphic position, timing, and duration of unconformities. These refinements provide a much more reliable framework for interpretation of biotic and paleoceanographic changes that occurred during the last 10 m.y. of the Cretaceous Period as observed on the Blake Nose.

The relative order and timing of a majority of the planktonic foraminiferal and calcareous nannofossil datum events identified at the Blake Nose sites show very good agreement among sites. Exceptions among the planktonic foraminifera include the zonal marker species *Globotruncana aegyptiaca* and *Gansserina gansseri*, which both have rare and sporadic distributions at the Blake Nose drill sites. Because recognition of the *G. gansseri* and *G. aegyptiaca* Zones is deemed unreliable, we define a new *Pseudoguembelina palpebra* Interval Zone for biostratigraphic subdivision between the *Globotruncanella havanensis* Partial-range Zone and the *Racemiguembelina fructicosa* Partial-range Zone. The FAD of *P. palpebra* is calibrated as 71.64 Ma. Secondary planktonic foraminiferal datum ages that are estimated from mean values obtained from the Blake Nose age models include: (1) the LAD of *Gansserina gansseri* = 65.93 Ma, (2) the LAD of *Contusotruncana patelliformis* = 66.20, (3) the LAD of *Globotruncana linneiana* = 67.86 Ma, (4) the LAD of *Globotruncana bulloides* = 68.80 Ma, (5) the LAD of *Contusotruncana fornicata* = 68.98 Ma, (6) the FAD of *Pseudotextularia elegans* = 69.02 Ma, (7) the FAD of *Planoglobulina acervulinoides* = 69.55 Ma, (8) the FAD of *Contusotruncana contusa* = 70.5 Ma, (9) the FAD of *Pseudoguembelina kempensis* = 71.50 Ma, (10) the FAD of *Racemiguembelina powelli* = 70.98 Ma and (11) the FAD of *Pseudoguembelina excolata* = 74.40 Ma.

Revision of the late Campanian-Maastrichtian chronology for the Blake Nose sites has an important bearing on paleoceanographic interpretations that have been made based on data generated from the drill cores and in correlation with data from other regions. Of particular interest is determination whether reorganization of the sources and patterns of deep- and intermediate-water circulation played a role in biotic changes, particularly the extinction of inoceramid bivalves. The extinction of inoceramid bivalves is now dated between 68.5 and 68.7 Ma on the Blake Nose. Combined stable isotope datasets published for the Blake Nose sites do not show any significant change in foraminiferal, bulk- and fine–fraction-carbonate $\delta^{18}O$ and $\delta^{13}C$ values in this interval.

The new chronology also provides reliable constraints on the timing and duration of Late Cretaceous unconformities across the Blake Nose transect. A mid-Maastrichtian unconformity with a duration ranging between 0.7 and 1.9 m.y. is identified at all three sites across the 1300-m-depth transect. Several additional unconformities occur within the upper Campanian, and the oldest of these spans the period from 10.2 to 34.4 m.y. The more precise age dating of these unconformities will provide a framework for understanding their cause and regional to global extent.

ACKNOWLEDGMENTS

This research used samples and data provided by the Integrated Ocean Drilling Program (IODP). IODP is sponsored by the U. S. National Science Foundation (NSF) and participating countries under management of the Joint Oceanographic Institutions (JOI), Inc. We extend our thanks to Jean Self-Trail (U. S. Geological Survey) for providing unpublished calcareous nannofossil biostratigraphic data and for training BTH in identification of some Maastrichtian species; Jim Ogg (Purdue University) for advice on correlation between Cretaceous biostratigraphic datums and the 2004 geomagnetic time scale; John McArthur for permission to use LOWESS version 4B; and to the CHRONOS System for developing and providing online access to the Age-depth Profile tool. This study benefited from reviews by R. K. Olsson and an anonymous reviewer and editorial suggestions by C. Brunner and M. R. Petrizzo.

REFERENCES

ABRAMOVICH, S., ALMOGI-LABIN, A., and BENJAMINI, C., 1998, Decline of the Maastrichtian pelagic exosystem based on planktic foraminifera assemblage change: implication for the terminal Cretaceous faunal crisis: Geology, v. 26, p. 63–66.

———, and KELLER, G., 2002, High stress late Maastrichtian paleoenvironment; inference from planktonic foraminifera in Tunisia: Palaeogeography, Palaeoclimatology, Palaeoecology, v. 178, p. 145–164. doi: 10.1016/S0031-0182(01)00394-7.

ARENILLAS, I., ARZ, J. A., MOLINA, E., and DUPUIS, C., 2000, The Cretaceous/Paleogene (K/P) boundary at Aïn Settara, Tunisia: sudden catastrophic mass extinction in planktic foraminifera: Journal of Foraminiferal Research, v. 30, p. 202–218.

ARZ, J. A., ARENILLAS, I., MOLINA, E., and SEPÚLVEDA, R., 2000, La estabilidad evolutiva de los foraminíferos planctónicos en el Maastrichtiense Superior y su extinción en el límite Cretácico/Terciario de Caravaca, España: Revista Geológica de Chile, v. 27, p. 27–47.

———, ———, SORIA, A. R., ALEGRET, L., GRAJALES-NISHIMURA, J. M., LIESA, C. L., MELÉNDEZ, A., MOLINA, E., and ROSALES, M. C., 2001, Micropaleontology and sedimentology across the Cretaceous/Tertiary boundary at La Ceiba (Mexico): impact-generated sediment gravity flows: Journal of South American Earth Sciences, v. 14, p. 505–519.

BARRERA, E., and SAVIN, S. M., 1999, Evolution of late Campanian-Mastrichtian marine climates and oceans, *in* Barrera, E., and Johnson, C. (eds.), Evolution of the Cretaceous Ocean-Climate System: Geological Society of America Special Paper 332, Boulder, CO, p. 245–282.

BELLIER, J.-P., MOULLADE, M., and HUBER, B. T., 2000, Mid-Cretaceous Planktonic Foraminifers from Blake Nose: revised biostratigraphic framework, *in* Kroon, D., Norris, R. D., and Klaus, A. (eds.), Proceedings of the Ocean Drilling Program, Scientific Results, 171B, [Online] Available from World Wide Web: <http://www-odp.tamu.edu/publications/171B_SR/chap_03/chap, 2007/10/5.

BENSON, W. E., SHERIDAN, R. E., and OTHERS. (eds.), 1978, Initial Reports of the Deep Sea Drilling Project, v. 44: U.S. Government Printing Office, Washington, D.C., 1005 p.

CANDE, S. C., and KENT, D. V., 1995, Revised calibration of the geomagnetic polarity timescale for the Late Cretaceous and Cenozoic: Journal of Geophysical Research, v. 100, p. 6093–6095.

COURTILLOT, V., BESSE, J., VANDAMME, D., MONTIGNY, R., JAEGER, J.-J., and CAPPETTA, H., 1986, Deccan flood basalts at the Cretaceous/Tertiary boundary?: Earth and Planetary Science Letters, v. 80, p. 361–374.

ERBA, E., PREMOLI SILVA, I., and WATKINS, D. K., 1995, Cretaceous calcareous plankton biostratigraphy of Sites 872 through 879, *in* Haggerty, J. A., Premoli Silva, I., Rack, F., and McNutt, M. K. (eds.), Proceedings of the Ocean Drilling Program, Scientific Results, v. 144: Ocean Drilling Program, College Station, Texas, p. 157–169.

FRANK, T. D., and ARTHUR, M. A., 1999, Tectonic forcings of Maastrichtian ocean-climate evolution: Paleoceanography, v. 14, p. 103–117.

———, THOMAS, D. J., LECKIE, R. M., ARTHUR, M. A., BOWN, P. R., JONES, K., and LEES, J., 2005, The Maastrichtian record from Shatsky Rise (northwest Pacific): a tropical perspective on global ecological and oceanographic changes: Paleoceanography, v. 20, p. PA1008. doi:10.1029/2004PA001052.

FRIEDRICH, O., and HEMLEBEN, C., 2007, Early Maastrichtian benthic foraminiferal assemblages from the western North Atlantic (Blake Nose) and their relation to paleoenvironmental changes: Marine Micropaleontology, v. 62, p. 31–44.

———, HERRLE, J. O., KÖßLER, P., and HEMLEBEN, C., 2004, Early Maastrichtian stable isotopes: changing deep water sources in the North Atlantic?: Palaeogeography, Palaeoclimatology, Palaeoecology, v. 211, p. 171–184.

GRADSTEIN, F. M., OGG, J. G., and SMITH, A. G., 2004, A Geologic Time Scale 2004: Cambridge University Press, Cambridge, 589 p.

———, AGTERBERG, F. P., OGG, J. G., HARDENBOL, J., VAN VEEN, P., THIERRY, J., and HUANG, Z., 1994, A Mesozoic time scale: Journal of Geophysical Research, v. 99, p. 24,051–24,074.

HANSEN, H. J., TOFT, P., MOHABEY, D. M., and SURKAR, A., 1996, Lameta age: dating the main pulse of the Deccan Traps volcanism: Gondwana Geology Magazine, v. 2, p. 365–374.

HARDENBOL, J., THIERRY, J., FARLEY, M.-B., DE GRACIANSKY, P. C., and VAIL, P. R., 1998, Mesozoic and Cenozoic sequence chronostratigraphic framework of European basins, *in* de Graciansky, P. C., Hardenbol, J., Thierry, J., and Vail, P. R. (eds.), Mesozoic and Cenozoic Sequence Stratigraphy of European Basins: Society for Sedimentary Geology (SEPM) Special Publication No. 60, p. 3–13.

HENRIKSSON, A. S., 1993, Biochronology of the terminal Cretaceous calcareous nannofossil zone of *Micula prinsii*: Cretaceous Research, v. 14, p. 59–68.

HUBER, B. T., 1990, Maestrichtian planktonic foraminifer biostratigraphy of the Maud Rise (Weddell Sea, Antarctica): ODP Leg 113 Holes 689B and 690C, *in* Barker, P. F., Kennett, J. P., and others. (eds.), Proceedings of the Ocean Drilling Program, Scientific Results, v. 113: Ocean Drilling Program, College Station, TX, p. 489–513.

———, and WATKINS, D. K., 1992, Biogeography of Campanian-Maastrichtian calcareous plankton in the region of the Southern Ocean: paleogeographic and paleoclimatic implications, *in* Kennett, J. P., and Warnke, D. A. (eds.), The Antarctic Paleoenvironment: A Perspective on Global Change, Antarctic Research Series, v. 56: American Geophysical Union, Washington, D.C., p. 31–60.

———, NORRIS, R. D., and MACLEOD, K. G., 2002, Deep sea paleotemperature record of extreme warmth during the Cretaceous: Geology, v. 30, p. 123–126.

ISAZA-LONDOÑO, C., MACLEOD, K. G., and HUBER, B. T., 2006, Maastrichtian North Atlantic warming, increasing stratification, and foraminiferal paleobiology at three timescales: Paleoceanography, v. 21, p. 1–10, PA1012. doi:10.1029/2004PA001130.

JARVIS, I., MABROUK, A., MOODY, R. T. J., and DE CABRERA, S., 2002, Late Cretaceous (Campanian) carbon isotope events, sea-level change and correlation of the Tethyan and Boreal realms: Palaeogeography, Palaeoclimatology, Palaeoecology, v. 188, p. 215–248.

KELLER, G., 1988, Extinction, survivorship and evolution of planktic foraminifers across the Cretaceous/Tertiary boundary at El Kef, Tunisia: Marine Micropaleontology, v. 13, p. 239–263.

———, 2004, Low-diversity, late Maastrichtian and early Danian planktic foraminiferal assemblages of the eastern Tethys: Journal of Foraminiferal Research, v. 34, p. 49–73.

———, BARRERA, E., SCHMITZ, B., and MATTSON, E., 1993, Gradual mass extinction, species survivorship, and long-term environmental changes across the Cretaceous-Tertiary boundary in high latitudes: Geological Society of America Bulletin, v. 105, p. 979–997.

KLAUS, A., NORRIS, R. D., KROON, D., and SMIT, J., 2000, Impact-induced mass wasting at the K-T boundary: Blake Nose, western North Atlantic: Geology, v. 28, p. 319–322.

KUCERA, M., and MALMGREN, B. A., 1996, Latitudinal variation in the planktic foraminifer *Contusatruncana contusa* in the terminal Cretaceous ocean: Marine Micropaleontology, v. 28, p. 31–52.

LI, L., and KELLER, G., 1998, Maastrichtian climate, productivity and faunal turnovers in planktic foraminifera in South Atlantic DSDP sites 525A and 21: Marine Micropaleontology, v. 33, p. 55–86.

———, and ———, 1999, Variability in Late Cretaceous climate and deep waters: evidence from stable isotopes: Marine Geology, v. 161, p. 171–190.

MACLEOD, K. G., 1994, Bioturbation, inoceramid extinction, and mid-Maastrichtian ecological change: Geology, v. 22, p. 139–142.

———, and HUBER, B. T., 1996, Reorganization of deep ocean circulation accompanying a Late Cretaceous extinction event: Nature, v. 380, p. 422–425.

———, and ———, 2001, The Maastrichtian record at Blake Nose (western Atlantic) and implications for global paleoceanographic and biotic changes, *in* Kroon, D., Norris, R. D., and Klaus, A. (eds.), Western North Atlantic Palaeogene and Cretaceous Palaeoceanography: Geological Society of London, Special Publications, no. 183, p. 111–130.

———, FULLAGAR, P., and HUBER, B. T., 2003, $^{87}Sr/^{86}Sr$ test of the degree of impact-induced slope failure in the Maastrichtian of the western North Atlantic: Geology, v. 31, p. 311–314.

———, HUBER, B. T., and DUCHARME, M. L., 2000, Paleontological and geochemical constraints on changes in the deep ocean during the Cretaceous greenhouse interval, *in* Huber, B. T., MacLeod, K. G., and Wing, S. L. (eds.), Warm Climates in Earth History: Cambridge University Press, Cambridge, p. 241–274.

———, ———, and FULLAGAR, P. D., 2001a, Evidence for a small (~0.000030) but resolvable increase in seawater $^{87}Sr/^{86}Sr$ ratios across the Cretaceous-Tertiary boundary: Geology, v. 29, p. 303–306.

———, ———, and ISAZA-LONDOÑO, C., 2005, North Atlantic warming during global cooling at the end of the Cretaceous: Geology, v. 33, p. 437–440.

———, WHITNEY, D., HUBER, B. T., and KOEBERL, C., 2007, Impact and extinction in remarkably complete K/T boundary sections from Demerara Rise, tropical western North Atlantic: Bulletin of the Geological Society of America, v. 119, p. 101–115.

———, HUBER, B. T., PLETSCH, T., RÖHL, U., and KUCERA, M., 2001b, Maastrichtian foraminiferal and paleoceanographic changes on Milankovitch time scales: Paleoceanography, v. 16, p. 133–154.

MASTERS, B. A., 1976, Planktonic foraminifera from the upper Cretaceous Selma group, Alabama: Journal of Paleontology, v. 50, p. 318–330.

MCARTHUR, J. M., and HOWARTH, R. J., 2004, Strontium isotope stratigraphy, *in* Ogg, J. G., Gradstein, F. M., and Smith, A. G. (eds.), Geological Timescale 2004: Cambridge University Press, Cambridge, p. 1–589.

MILLER, K. G., WRIGHT, J. D., and BROWNING, J. V., 2005, Visions of ice sheets in a greenhouse world: Marine Geology, v. 217, p. 215–231.

———, BARRERA, E., OLSSON, R. K., SUGARMAN, P. J., and SAVIN, S. M., 1999, Does ice drive early Maastrichtian eustasy?: Geology, v. 27, p. 783–786.

MOLINA, E., ALEGRET, L., ARENILLAS, I., and ARZ, J. A., 2005, The Cretaceous/Paleogene boundary at the Agost section revisited: paleoenvironmental reconstruction and mass extinction pattern: Journal of Iberian Geology, v. 31, p. 135–148.

MONECHI, S., and THIERSTEIN, H. R., 1985, Late Cretaceous-Eocene nannofossil and magnetostratigraphic correlations near Gubbio, Italy: Marine Micropaleontology, v. 9, p. 419–440.

NASH, S., 1981, A neotype for the Cretaceous genus *Pseudotextularia* Rzehak, 1891: Journal of Foraminiferal Research, v. 11, p. 70–75.

NEDERBRAGT, A. J., 1991, Late Cretaceous biostratigraphy and development of Heterohelicidae (planktic foraminifera): Micropaleontology, v. 37, p. 329–372.

NORRIS, R. D., and FIRTH, J., 2001, Mass wasting of Atlantic continental margins following the Chicxulub impact event, *in* Koeberl, C., and MacLeod, K. G. (eds.), Catastrophic Events and Mass Extinctions: Impacts and Beyond: Geological Society of America, Special Paper 356, p. 79–95.

———, HUBER, B. T., and SELF-TRAIL, J., 1999, Synchroneity of the K-T oceanic mass extinction and meteorite impact: Blake Nose, western North Atlantic: Geology, v. 27, p. 419–422.

———, KROON, D., and KLAUS, A. (eds.) 1998, Proceedings of the Ocean Drilling Program, Initial Reports, v. 171B: Ocean Drilling Program, College Station, TX, 749 p.

———, FIRTH, J., BLUSZTAJN, J. S., and RAVIZZA, G., 2000, Mass failure of the North Atlantic margin triggered by the Cretaceous-Paleogene bolide impact: Geology, v. 28, p. 1119–1122.

OGG, J. G., and BARDOT, L., 2001, Aptian through Eocene magnetostratigraphic correlation of the Blake Nose transect (Leg 171B), Florida continental margin, *in* Kroon, D., Norris, R. D., and Klaus, A. (eds.), Proceedings of the Ocean Drilling Program, Scientific Results, v. 171B: Ocean Drilling Program, College Station, Texas, p. 1–59 [CD-ROM].

OLSSON, R. K., WRIGHT, J. D., and MILLER, K. G., 2001, Paleobioeography of *Pseudotextularia elegans* during the latest Maastrichtian global warming event: Journal of Foraminiferal Research, v. 31, p. 275–282.

PERCH-NIELSEN, K., 1985, Mesozoic calcareous nannofossils, *in* Bolli, H. M., Saunders, J. B., and Perch-Neilsen, K. (eds.), Plankton Stratigraphy: Cambridge University Press, Cambridge, p. 329–426.

PETRIZZO, M. R., and HUBER, B. T., 2006, Biostratigraphy and taxonomy of late Albian planktonic foraminifera from ODP Leg 171B (western North Atlantic Ocean): Journal of Foraminiferal Research, v. 36, p. 166–190.

POSPICHAL, J. J., and WISE, S. W., JR., 1990, Maestrichtian calcareous nannofossil biostratigraphy of Maud Rise ODP Leg 113 Sites 689 and 690, Weddell Sea, *in* Barker, P. F., Kennett, J. P., and others. (eds.), Proceedings of the Ocean Drilling Program, Scientific Results, v. 113: Ocean Drilling Program, College Station, TX, p. 465–487.

PREMOLI SILVA, I., and SLITER, W. V., 1994, Cretaceous planktonic foraminiferal biostratigraphy and evolutionary trends from the Bottaccione section, Gubbio, Italy: Palaeontographia Italica, v. 82, p. 1–89.

ROBASZYNSKI, F., and CARON, M., 1995, Foraminifères planktoniques du Crétacé: commentaire de la zonation Europe-Mediterranée: Société géologique de France, v. 166, p. 681–692.

SELF-TRAIL, J. M., 2001, Biostratigraphic subdivision and correlation of upper Maastrichtian sediments from the Atlantic Coastal Plain and Blake Nose, Western Atlantic, *in* Kroon, D., Norris, R. D., and Klaus, A. (eds.), Western North Atlantic Palaeogene and Cretaceous Palaeoceanography: Geological Society of London, Special Publication 183, London, p. 93–110.

———, 2002, Trends in late Maastrichtian calcareous nannofossil distribution patterns, Western North Atlantic margin: Micropaleontology, v. 48, p. 31–52.

SHIPBOARD SCIENTIFIC PARTY., 2004, Explanatory notes, *in* Erbacher, J., Mosher, D. C., Malone, M. J., and others. (eds.), Proceedings of the Ocean Drilling Program, Initial Reports, v. 207: Ocean Drilling Program, College Station, Texas, p. 1–94. doi:10.2973/odp.proc.ir.207.2004.

SISSINGH, W., 1977, Biostratigraphy of Cretaceous calcareous nannoplankton: Geologie en Mijnbouw, v. 56, p. 37–50.

WATKINS, D. K., and SELF-TRAIL, J. M., 2005, Calcareous nannofossil evidence for the existence of the Gulf Stream during the late Maastrichtian: Paleoceanography, v. 20, p. PA3006. doi:10.1029/2004PA001121.

WILF, P., JOHNSON, K. R., and HUBER, B. T., 2003, Correlated terrestrial and marine evidence for global climate changes before mass extinction at the Cretaceous-Paleogene boundary: Proceedings of the National Academy of Sciences, v. 100, p. 599–604.

WONDERS, A. A. H., 1980, Middle and Late Cretaceous planktonic foraminifera of the western Mediterranean area: Utrecht Micropaleontology Bulletin, v. 24, p. 1–158.

Received 4 October 2007
Accepted 19 November 2007